A step towards functional aqueous super-lubricity.

Emily McNulty, Chris Collinson and Thomas Cracknell

Mini Project Group 5

University of Leeds

Supervisor: Dr Michael Bryant

Abstract

Natural synovial joints display extremely favourable tribological characteristics, extremely low friction and wear. It is postulated poroelasticity is one of the mechanisms responsible for these properties.[1] Microporous PDMS was prepared using a templating technique with heat sintered PMMA beads. Compression tests were carried out using a Mecmesin compressor and a load cell of 10 N. Tribological tests were completed under a range of conditions using both a bespoke tribometer and an Anton Paar NTR^3 nano-tribometer with either water or glycerol as a lubricant. Although the porous samples did not exhibit significant poroelastic behaviour with aqueous lubrication, using glycerol as a lubricant did result in the porous samples demonstrating poroelastic properties, halving the frictional coefficient as compared with water, and under some sliding conditions reducing the frictional coefficient to as low as 0.15.

Table of Contents

1 Introduction

With an ever increasing need to reduce the friction and wear of machines, work has turned towards bio-inspiration in order to improve tribological systems (2). Joints from the biological world, such as the knee and hip joints, provide a considerable amount of inspiration for tribologists as they combine the important properties needed for tribological systems. These properties include; extremely low coefficients of friction, very low rates of wear – with a working lifetime of up to 70 years, and the ability to withstand high loads. As such a combination of properties has not yet been achieved with conventional tribological materials and systems, it is hoped that a biomimetic approach will have a better success in achieving a similar performance to natural synovial joints (3). These joints can exhibit coefficients of friction as low as 0.002-0.006, which is remarkable, considering the fluid viscosities, loads and speeds encountered (2).

There are numerous theories and much debate over the exact mechanisms of synovial joints and how such low frictional coefficients are achieved, however what is clear is that some of the load through the joint is supported by pressurisation of the fluid in the surface & interface (2, 4, 5). Due to the pressurisation of the fluid, the two surface remain separated and thus as the surfaces move it is the synovial fluid that shears rather than the surfaces, ergo the very low friction coefficient (6).

A poroelastic material is constituted of a solid porous matrix which is elastic, and a viscous fluid within the pores (4, 5, 7). The theory of poroelasticity was primarily developed by Biot between 1935 and 1957 and states that as stress is applied to a porous material, the solid matrix deforms elastically, resulting in volumetric changes to the pores (4, 5, 7, 8). These volumetric changes to pore size result in pressurisation of the fluid, resulting in flow of pore fluid from areas of high pressure to low pressure (9). The flow rate of the pore fluid depends on the fluid viscosity, and can be modelled using Darcy's law (4, 7, 9).

Undoubtedly a poroelastic material will have a high compressive modulus due to the stiffening effect of the fluid pores (4, 5, 7), thus such a material could support a practical load in a tribological system (2, 6). In addition to this the pressurisation of the fluid in surface pores due to loading results in a repulsive hydrodynamic force on the contact. Thus resulting in hydrodynamic lubrication, even at relatively low sliding speeds (2, 6).

The large variety of applications of porous polymeric materials, has led to a great interest in the design of these materials (10). Processes for producing porous polymeric materials have been developed, by using suitable polymer templates. These templates are able to produce the specific pores needed within the polymeric material. Another process for producing porous materials is via

the use of interpenetrating polymer networks (IPNs). An IPN can be described as a combination of two polymers in the form of a network, where one of the polymers has been synthesized in the presence of the other (10).

Hong, Y. *et al*. designed and produced a method to fabricate an interconnected porous elastomer, using monomers for a polyurethane elastomer, cast onto a microsphere template of sintered jojoba wax beads (11). A heat sintering (HS) process was used to sinter the jojoba wax beads, to create a microsphere template which was then covered with polyurethane elastomer. The beads were then removed from the polyurethane elastomer via a 'squeezing' method resulting in a porous polyurethane elastomer. Figure 1 shows the method to create the porous elastomer.

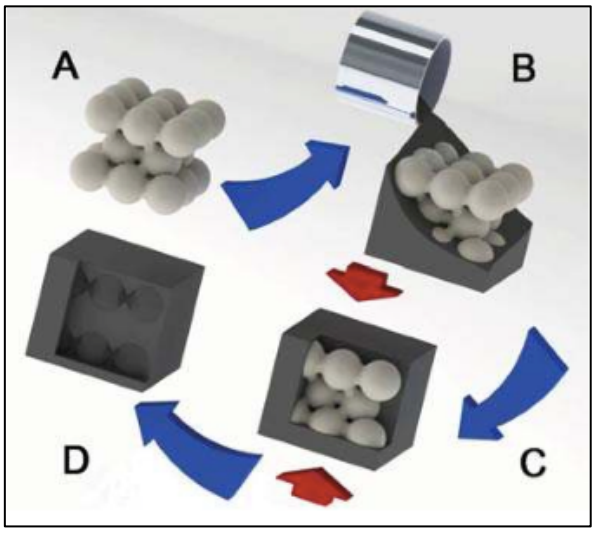

Figure 1. Diagram showing the fabrication of the porous elastomer. A) Jojoba wax bead template sintering, B) casting of polyurethane elastomer, C) removal of jojoba wax template, via the 'squeeze' method, D) resulting porous polyurethane elastomer.

Cam, C. and Segura, T. produced porous hyaluronic acid hydrogels using heat sintering (HS), non-sintering (NS) and chemical sintering (CS) methods of PMMA. Results showed that the CS method was the most favoured as it created a uniform porous structure, when compared to the HS and NS methods (12).

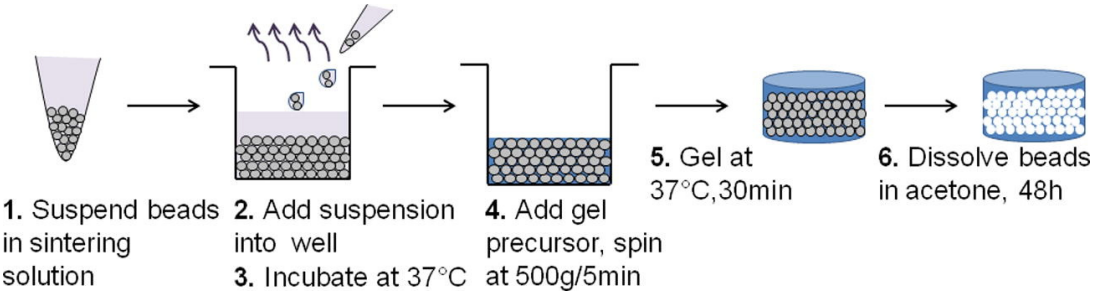

Figure 2. Schematic of formation of porous hyaluronic acid hydrogels, using a chemical sintering method.

Scanning electron microscope (SEM) images show the porous structure of the HS, NS and CS sintering methods (Figure 3). The chemical sintering method showed that the porous hyaluronic acid hydrogel had uniform pore interconnectivity and pore structure in comparison to the other two methods (12).

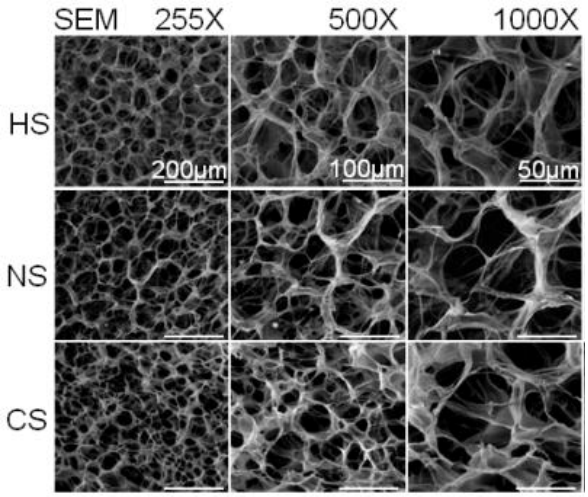

Figure 3. Scanning electron microscope images of heat sintered (HS), non-sintered (NS) and chemical sintered (CS) porous polyurethane elastomer.

2 Aims and Objectives

The aim of the project was to create a bearing system capable of providing low friction and wear across a range of suitable loading situations by using fluid pressurisation to support the loads. In order to do this, a multi-modulus poroelastic material will be fabricated, optimised and characterised so that it can be capable of functional aqueous lubrication. Once this has been achieved, a suitable method for testing the optimised low modulus material will be designed and developed.

3 Results and Discussion

3.1 Sample Preparation

3.1.1 Sintering of PMMA beads

Porous samples were prepared by sintering poly(methyl methacrylate) (PMMA) (Alfa Aesar PMMA powder) beads, using both a heat sintering and chemical sintering method, followed by the addition of a polydimethylsiloxane (PDMS) elastomer (Sylgard 184 kit, Dow Corning), which was heated in order to cure.

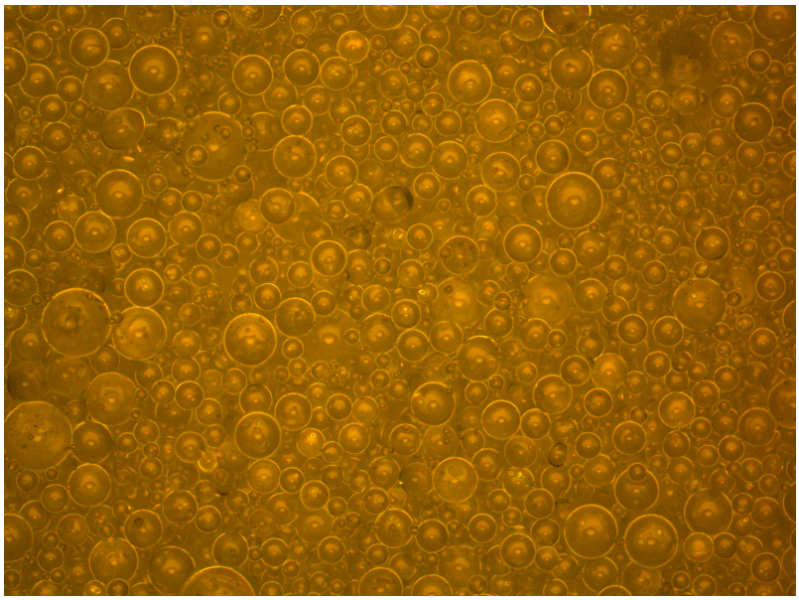

Figure 4. Heat sintered PMMA beads, image taken from the optical microscope.

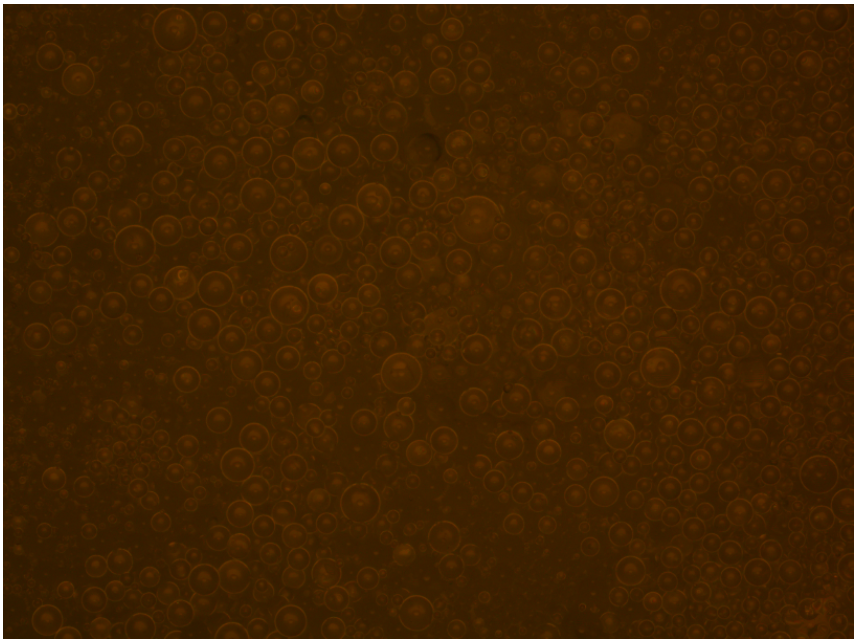

Figure 5. Non-sintered PMMA beads, image taken from the optical microscope.

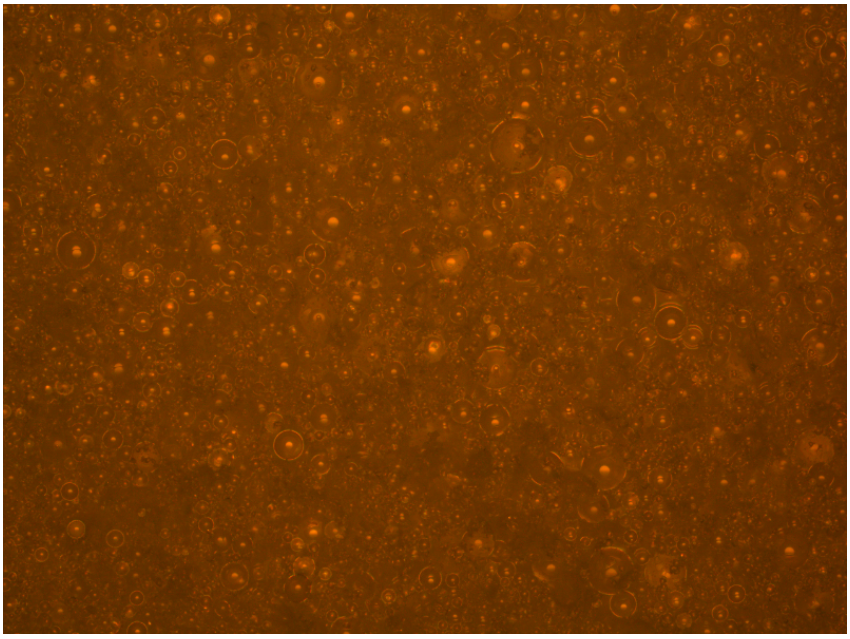

Figure 6. Chemically sintered PMMA beads, image taken from the optical microscope.

It was found that although the chemical sintering process worked, it was not entirely successful. Once the 1% acetone in 70% ethanol sintering solution had evaporated from the PMMA beads, the sample surface cracked and the PMMA beads pulled away from the edges of the aluminium ring. Thus leading to the sintered beads floating within the PDMS elastomer when it was added, as opposed to remaining in a uniform layer at the base of the sample. **Error! Reference source not found.** shows that the beads had indeed sintered, however some of the beads had deformed,

suggesting that chemical sintering is not appropriate. Due to this, the heat sintered method is the most appropriate as the beads do not pull away from the aluminium ring and remained as a uniform layer at the base of the sample. **Error! Reference source not found.** shows that the beads had sintered, this can be seen from the necks formed between beads. There was also little deformation of the beads for heat sintering compared to chemical. PDMS was not added to the non-sintered beads (**Error! Reference source not found.**), however optical microscope images were taken to compare the beads before and after sintering.

3.1.2 Addition of PDMS elastomer

It was found that the PDMS elastomer required a slight amount of vacuuming, in order to remove any air bubbles prior to the addition of PDMS to the PMMA sintered beads. The PDMS was vacuumed for 1 hour, which was a suitable amount of time to remove all the air bubbles present in the PDMS. On addition of PDMS to sintered PMMA beads, more air bubbles formed within the PDMS thus further vacuuming was required. The elastomer and beads were then vacuumed for a further 30 minutes to ensure there were no air bubbles present that could have an effect on the PDMS during curing.

3.1.3 Dissolving of PMMA beads

Once the PDMS had cured, the PMMA beads had to be removed. The literature suggested;

1. A squeezing method, which required heating, centrifugation and squeezing to remove the liquid beads from the elastomer;
2. Removal of the beads by dissolving the PMMA in acetone for 48 hours.

Samples were initially dissolved in acetone, and left at room temperature for 48 hours. On analysis of the samples using the optical microscope, a porous structure was not present therefore suggesting that the beads had not dissolved (Figure 7). Dichloromethane (DCM) and dimethylformamide (DMF) were also tested. DCM was not suitable for dissolving the PMMA beads as it affected and swelled the PDMS elastomer, however DMF was suitable as it did not have an effect on the PDMS. The samples were left to dissolve in DMF for 48 hours, and on analysis under the optical microscope a porous structure was present (Figure 8 and Figure 9).

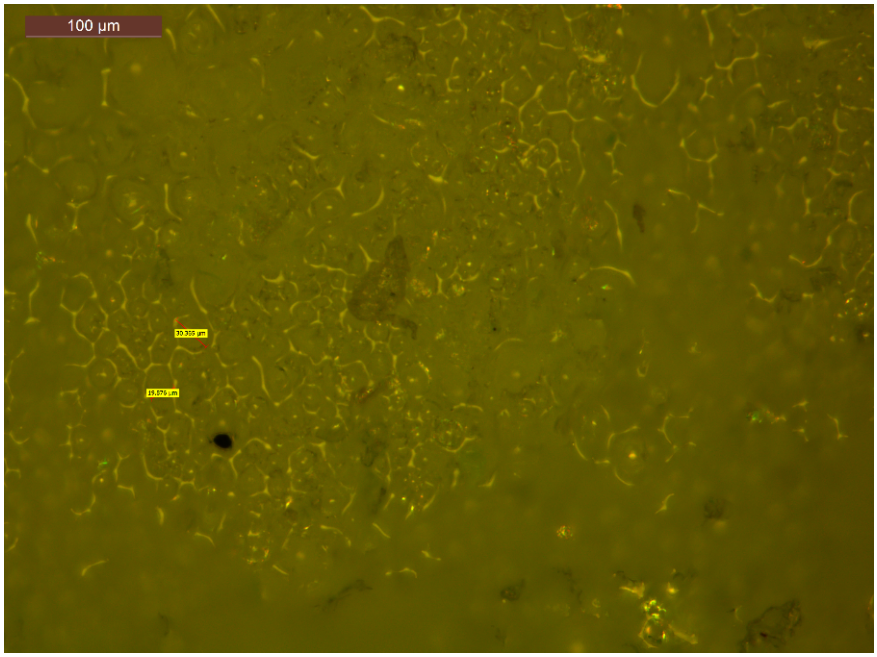

Figure 7. Optical microscope image of sample dissolved in acetone for 48 hours.

Figure 7 shows that the beads had only partly dissolved in the acetone, and due to regions that are blurred, the acetone may have also affected the PDMS elastomer.

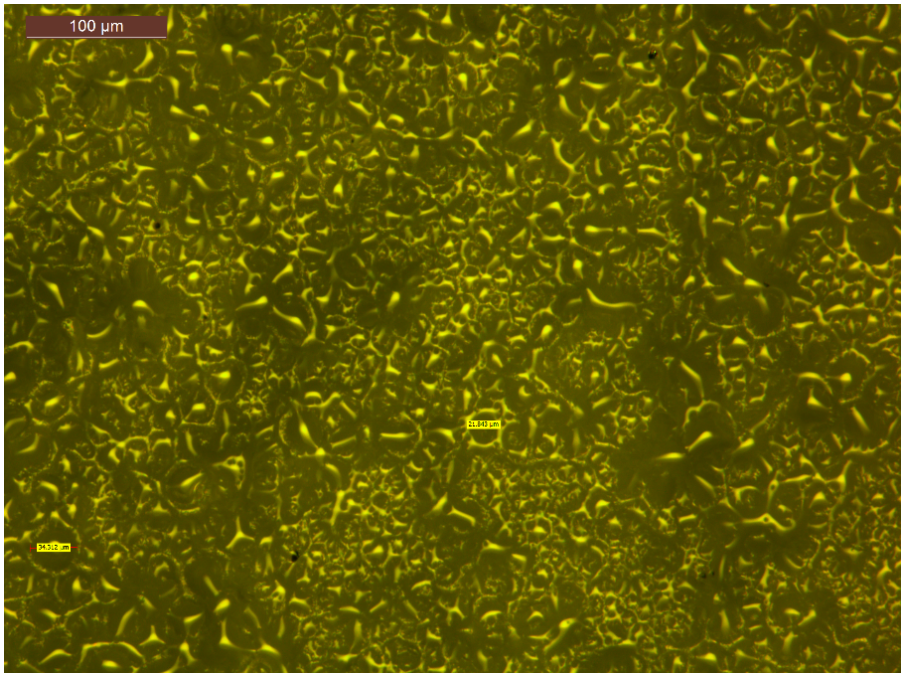

Figure 8. Optical microscope image of sample dissolved in dimethylformamide (DMF), 24 hours.

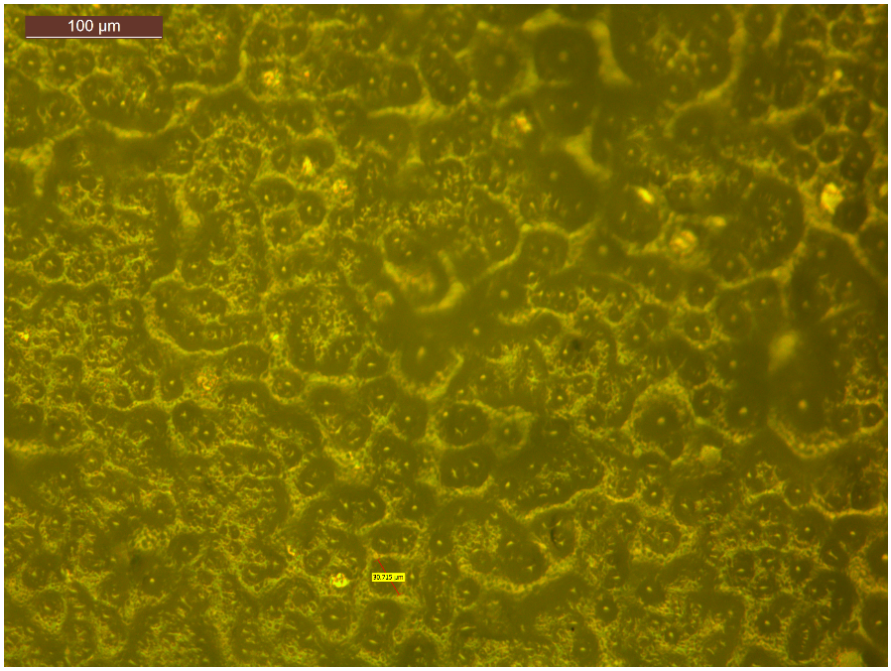

Figure 9. Optical microscope image of sample dissolved in dimethylformamide (DMF), 48 hours.

It can be seen from Figure 8 and Figure 9 that the beads had dissolved out of the PDMS elastomer as pores are present on the surface. Although the optical microscope was sufficient at showing a porous structure of the top layer of the sample, a more advanced method was used in order to investigate whether or not there was a porous structure throughout the sample. A computed tomography (CT) scan was performed and it showed that the samples had a porous structure throughout.

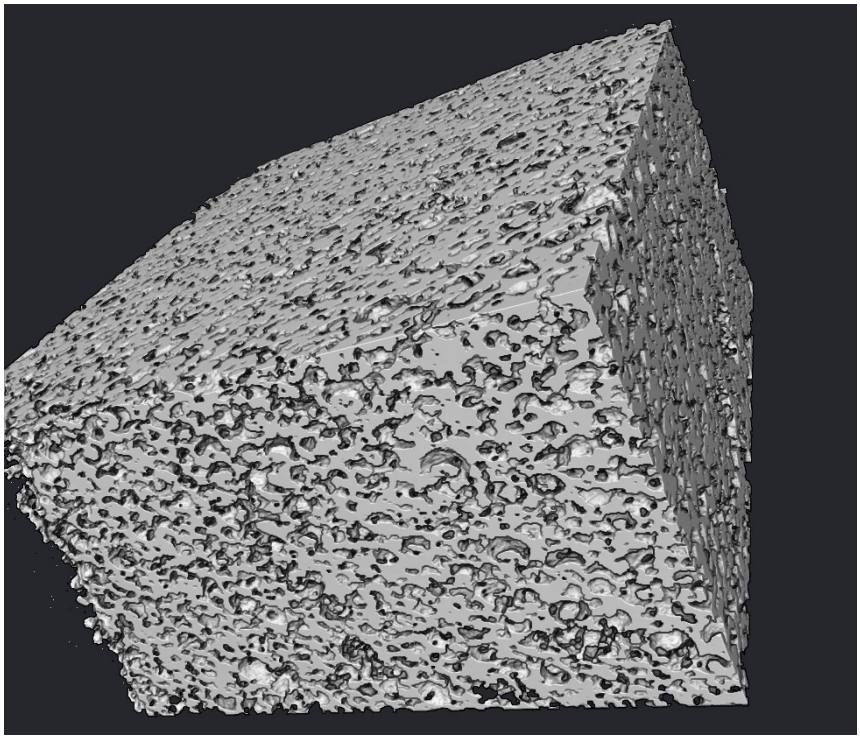

Figure 10. Computed tomography (CT) scan of the porous PDMS elastomer.

The porosity of the porous PDMS was calculated by comparing the weight of the porous sample against a bulk non-porous PDMS sample:

$$Weight\ of\ bulk = 2.04\ g, \qquad Weight\ of\ porous = 1.74\ g$$

$$Mass\ of\ porous\ area = 0.30\ g\ \rightarrow Volume\ of\ PDMS\ in\ porous\ area = 0.30\ cm^3$$

$$Volume\ of\ PMMA = \frac{1.0\text{g}}{1.18\ \text{gcm}^{-3}} = 0.85\ cm^3$$

$$Total\ volume\ of\ porous\ area = 0.85\ cm^3 + 0.3\ cm^3 = \ 1.15\ cm^3$$

$$\%\ Porosity = \frac{0.85\ cm^3}{1.15\ cm^3} = \ 74\ \%$$

The other alternative "squeeze" method for PMMA removal would be to heat up the samples to above the melting point of PMMA, approximately 160°C, and then mechanically squeeze or centrifuge the liquid PMMA out of the sample. However at such temperatures the PDMS elastomer may become unstable, even though below its melting temperature of approximately 300°C.

Once the microsphere template has been removed from the elastomer, the aqueous lubricant can be added. The samples will firstly be trialled with water only, and depending on the results the elastomer may be filled with a hydrogel to increase water retention.

3.2 Tribological Results

Initial results from the bespoke low load tribometer as seen in Figure 12Figure 11 gave frictional coefficients of bulk PDMS as μ=2.1 under dry conditions and μ=0.3 when lubricated with water. For porous PDMS lubricated with water the frictional coefficient was 0.9.

Results from the Anton Paar tribometer also showed the coefficient of friction in water for porous PDMS to be 0.8, much higher than that for bulk PDMS, as seen in Figure 13. Plasma treatment did slightly decrease the coefficient of friction for porous PDMS to around 0.65, however this is still substantially higher than 0.1 for the plasma treated bulk PDMS.

As shown in Figure 14, using glycerol as a lubricant resulted in a reduction in the frictional coefficient of porous PDMS, from 0.8 in water to 0.4 in glycerol. The frictional coefficient for the bulk PDMS in glycerol increased slightly by 0.05.

Varying the load resulted in the frictional coefficient decreasing in a linear relationship as load increased for porous PDMS, whereas for bulk PDMS friction remained somewhat constant until 70mN above which the frictional constant increases, as demonstrated in Figure 15.

Altering the sliding speed had inconclusive effects for the bulk PDMS samples. Conversely for the porous PDMS sample increasing the sliding speed dramatically reduces the frictional coefficient, reaching a value as low as 0.15 for some porous samples.

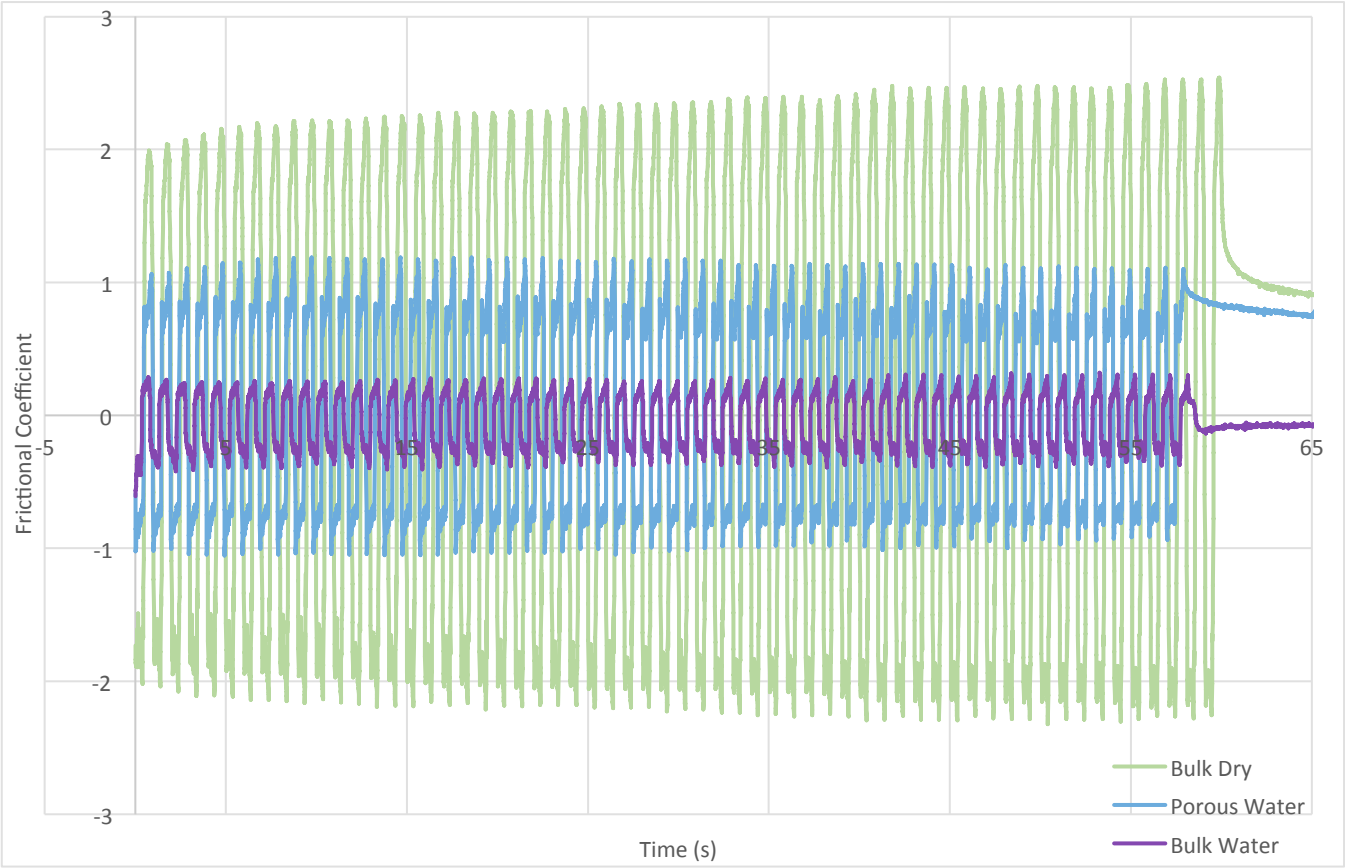

Figure 12. Frictional coefficient varying with time for a load of 3.2N and sliding speed of 4.44cm/s over a time period of 60s using the bespoke tribometer.

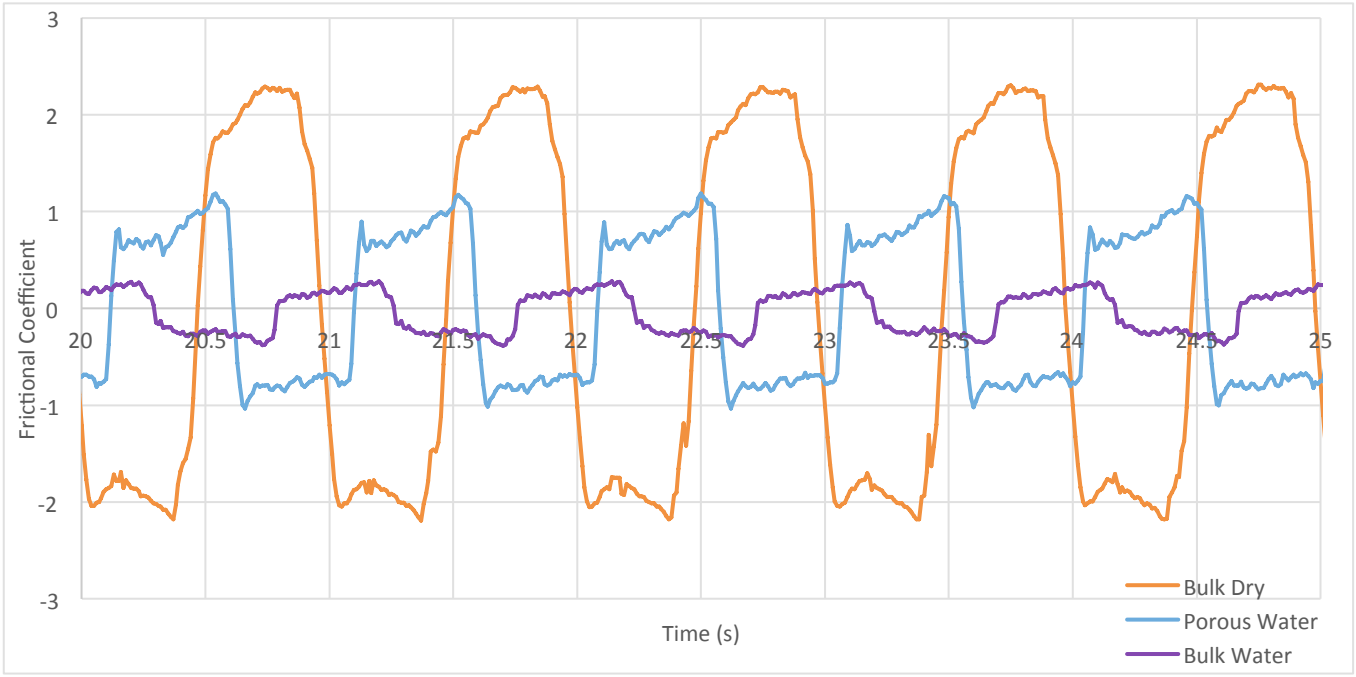

Figure 11. Detail of Figure 1 between 20 and 25s.

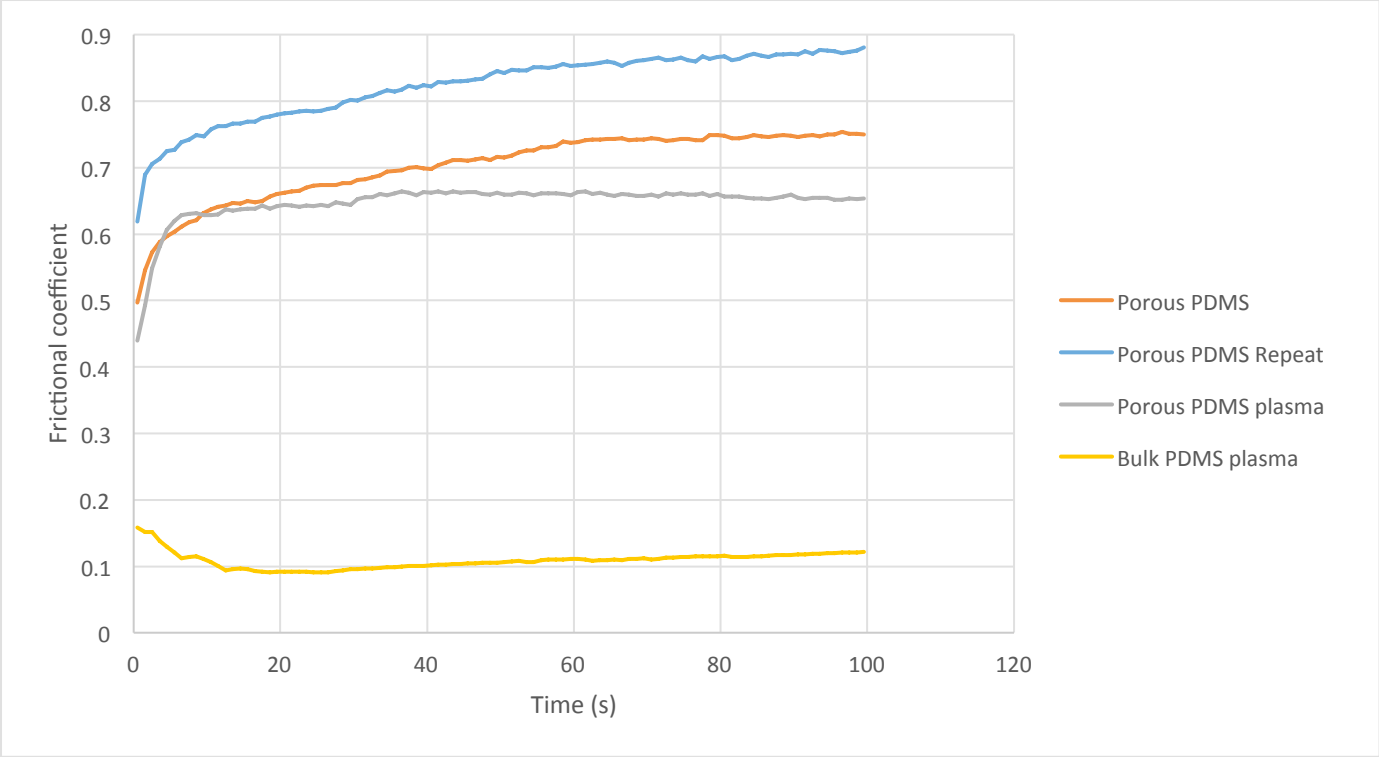

Figure 13. Evolution of the frictional coefficient with time for porous and bulk PDMS in water, before and after plasma treatment. Measured using Anton Paar tribometer with load of 100mN and sliding speed of 3140µm/s.

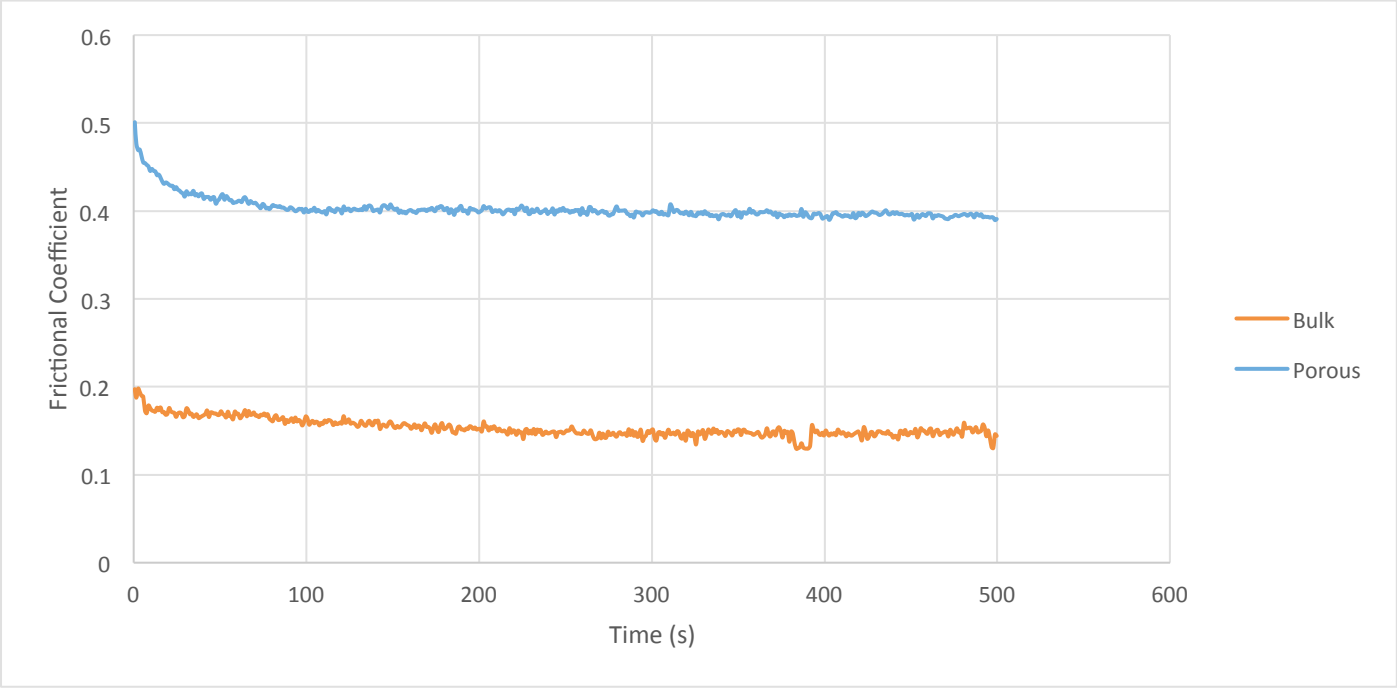

Figure 14. Variation of frictional coefficient with time for bulk and porous PDMS in glycerol using Anton Paar tribometer with load of 90mN and sliding speed of 2000µm/s.

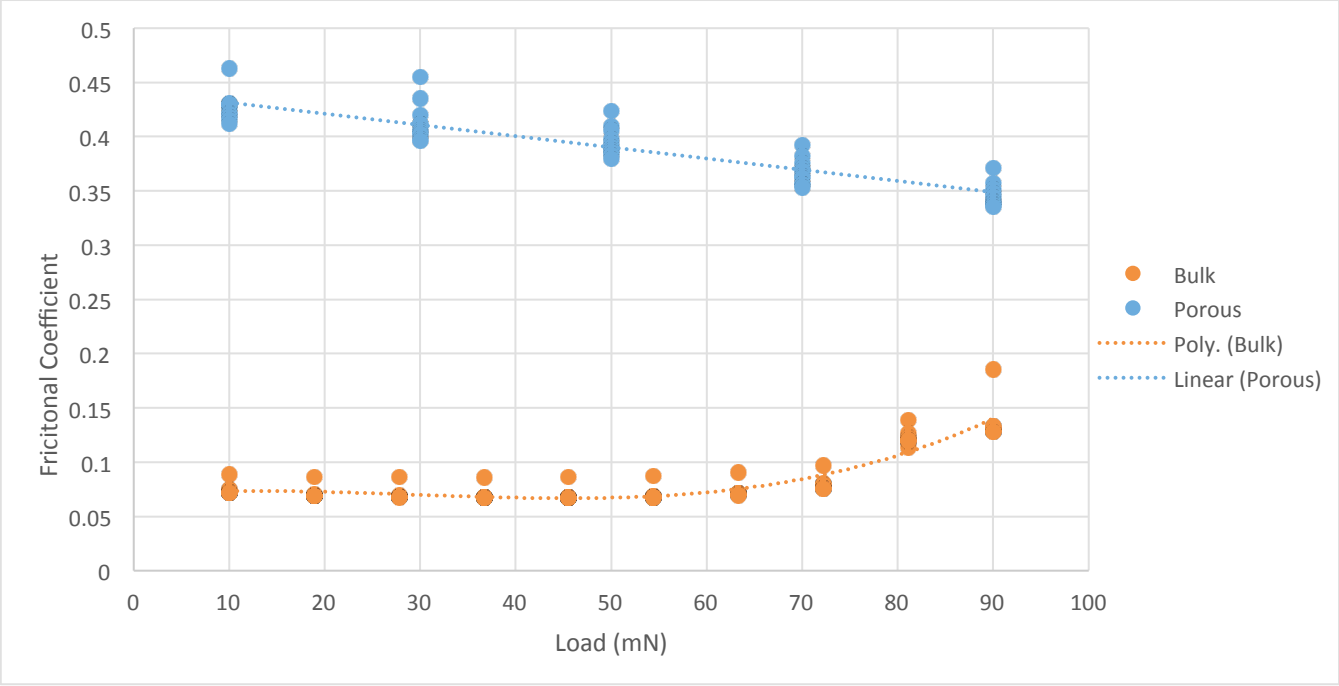

Figure 15. Variation of frictional coefficient with load for porous and bulk PDMS in glycerol using Anton Paar Tribometer with sliding speed of 1000µm/s.

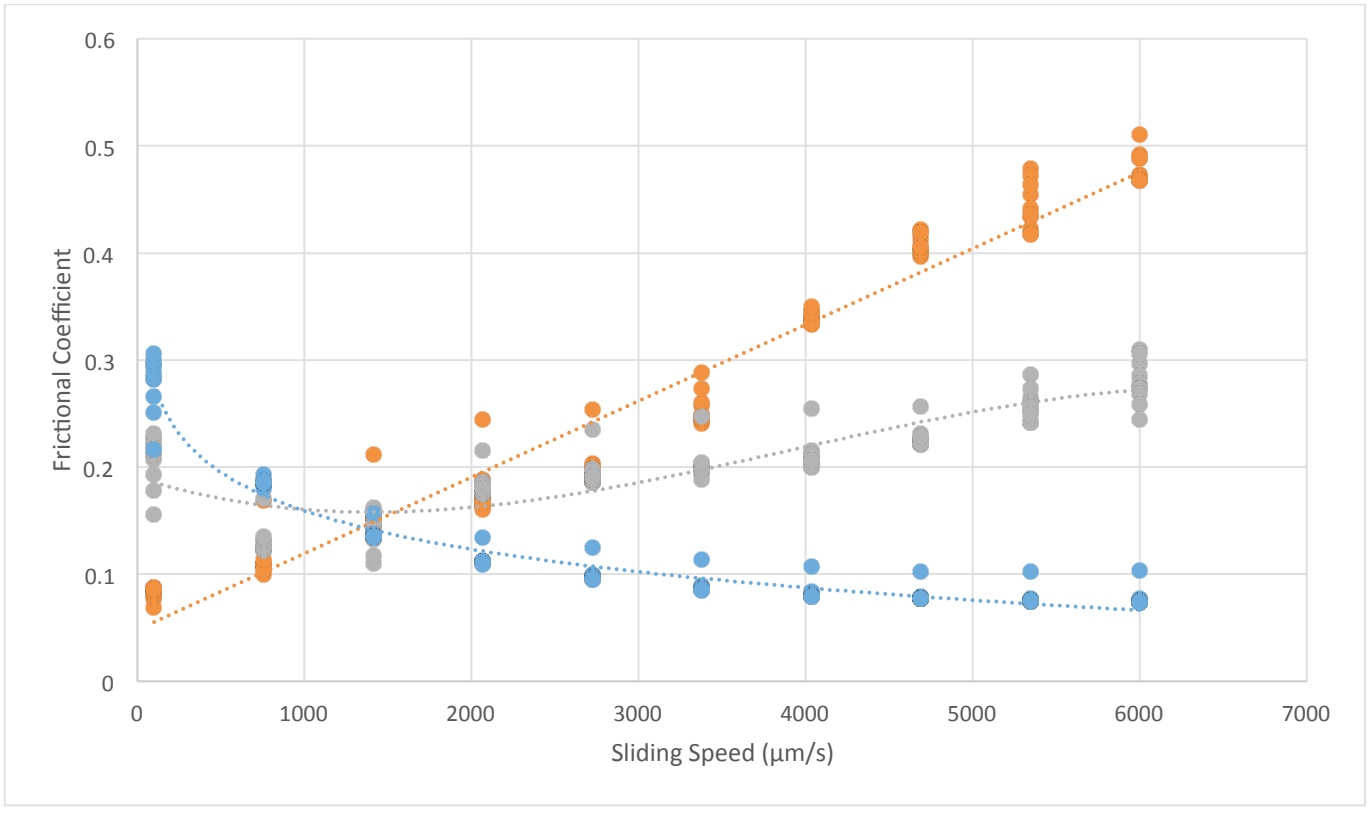

Figure 16. Evolution of frictional coefficient with sliding speed for bulk PDMS in glycerol using Anton Paar Tribometer with load of 90mN.

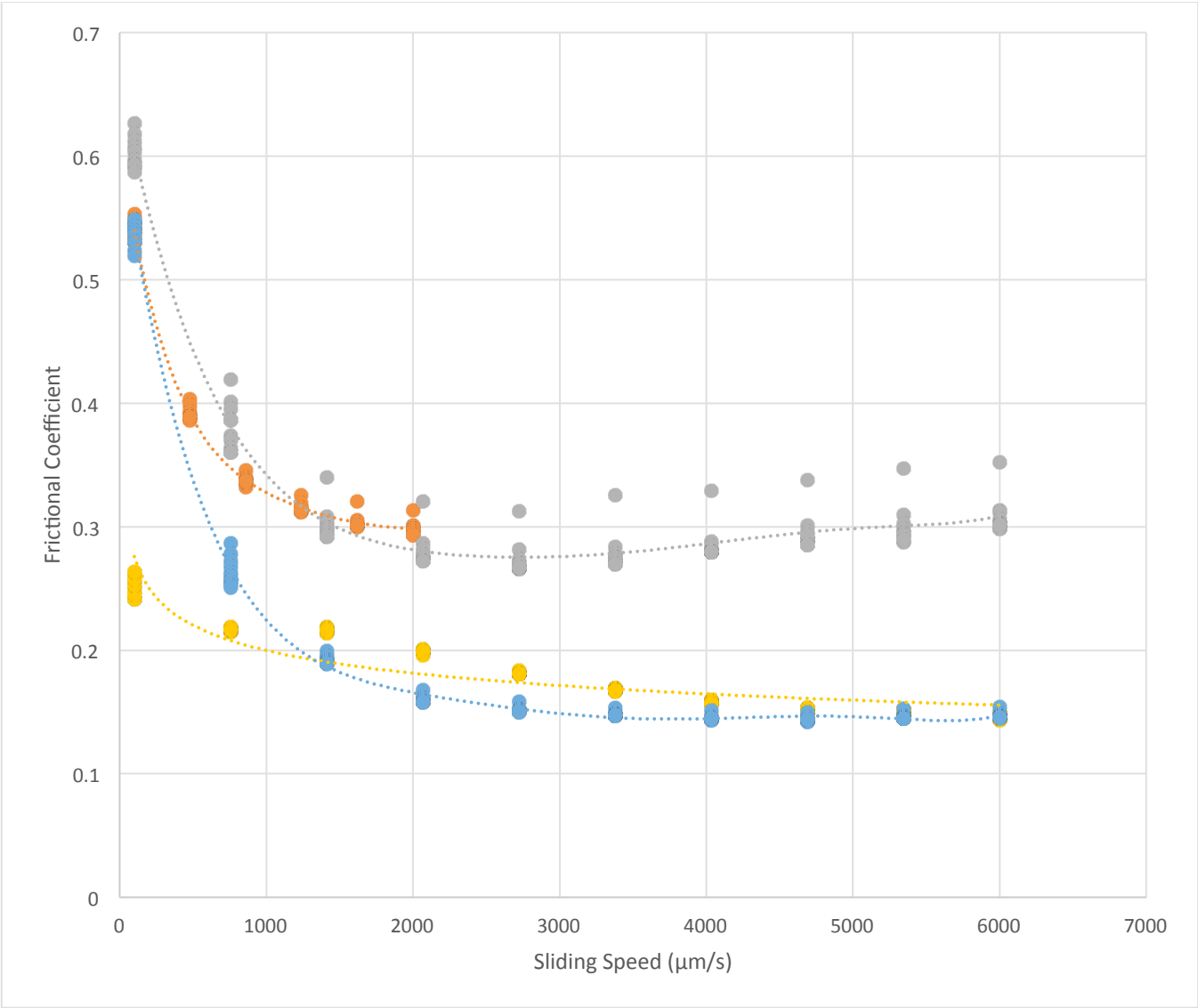

Figure 17. Frictional coefficient varying with sliding speed for porous PDMS in glycerol using Anton Paar Tribometer with load of 90mN.

Discussion

The initial results clearly show a frictional coefficient for the porous PDMS in water of around three times the coefficient for bulk PDMS in water. This is most likely due to the hydrophobic nature of PDMS. Due to the hydrophobicity it is unlikely that there is appreciable penetration of water into the micropores of the PDMS, and so the intended poroelastic behaviour does not materialize (13).

The micropores should reduce the conformity of the PDMS as compared to bulk PDMS, and thus reduce friction, even without poroelastic lubrication. However the porous PDMS has a lower compressive modulus and therefore the deformation in the contact region is larger than for the bulk PDMS. Due to the greater deformation, the conformity of the contact is much higher for the porous PDMS, thus accounting for the higher coefficient of friction. The porous nature of the surface also increases surface roughness and therefore friction (14).

Due to the high porosity of the porous samples and the low viscosity of water, it is likely that only an insignificant portion of the load is supported due to fluid pressurisation, thus leading to the high frictional coefficients of the porous PDMS, even when the surface is plasma treated (9).

Glycerol results in higher friction for the bulk samples as it has a higher viscosity than water. In comparison the higher viscosity of glycerol will increase the load supported by the liquid phase in the porous samples (4, 7), thus the separation between the surfaces is increased and friction is reduced for the porous samples.

At very low loads the poroelastic effect does not occur as the load is not high enough to induce fluid pressurisation. Consequently increasing the load reduces the frictional coefficient for the porous samples. By increasing the sliding speed for the porous samples it appears that hydrodynamic lubrication can be induced even at relatively low sliding speeds as shown by Figure 17 (9).

It was found that different areas of the surface had different porosities, resulting in different frictional coefficients. This was a major limitation of the investigation as it led to large variations in the data. It is likely that this is due to the PDMS seeping below the sintered beads before curing, resulting in some areas of the beads floating above the bottom of the mould.

Both the reduction in the coefficient of friction for porous PDMS as sliding speed increases (Figure 17) and the reduction as load increases Figure 15 agree with other literature on the lubricity of porous PDMS published by Khosla *et al* (6).

3.3 Indentation Results

Initial results from the indentation test showed somewhat promising results for the porous samples. It was found that the bulk PDMS reacted in a different manner to the Porous samples. The bulk material deformed as expected, the load was applied and held for the duration of the test without any further changes in displacement. This is what is expected for an elastic material such as PDMS. Figure 18 (a) below shows the elastic response of the bulk PDMS at a 5N load. Figure 18 (b) shows the ideal analytical response for an elastically loaded material.

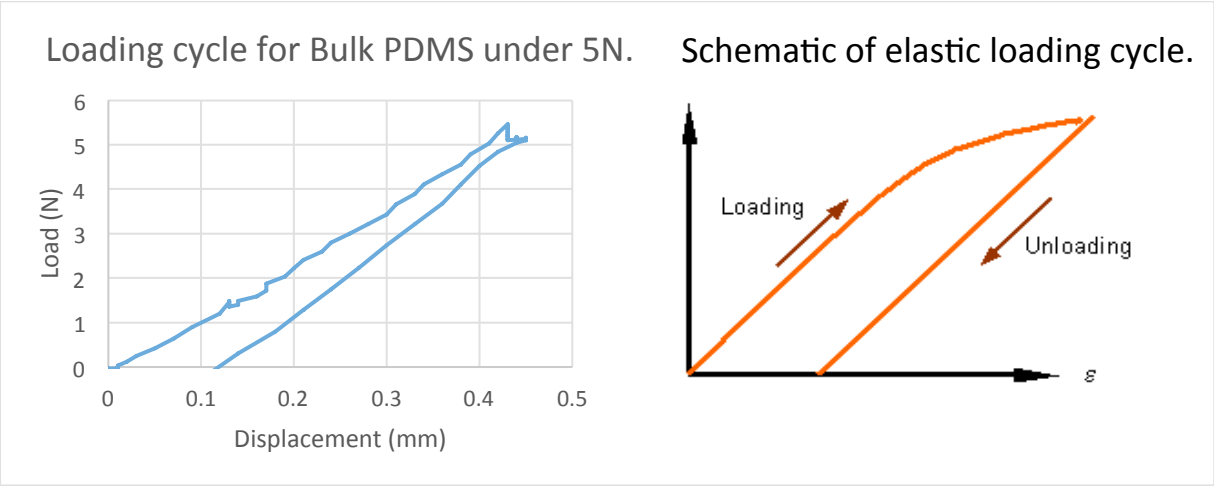

Figure 18. Loading cycle for Bulk modulus, recorded from indentation test (a) and schematic of elastic loading cycle (b) (1)

Where the displacement is not returning to the origin indicates there has viscoelastic behaviour. At low loads, it is unlikely that the PDMS will have deformed plastically due to its relatively high compressive modulus of between 0.8MPA and 2Mpa.(15).

While when the porous samples were tested, an increasing displacement was needed to maintain a constant force. This is what is expected of the porous samples as the load is taken by the lubricant within the pores before being displaced. Figure 19 below shows the comparison between the bulk and porous samples as they undergo 5N compression test.

Figure 19. A comparison of the loading cycles between the porous and bulk samples of PDMS.

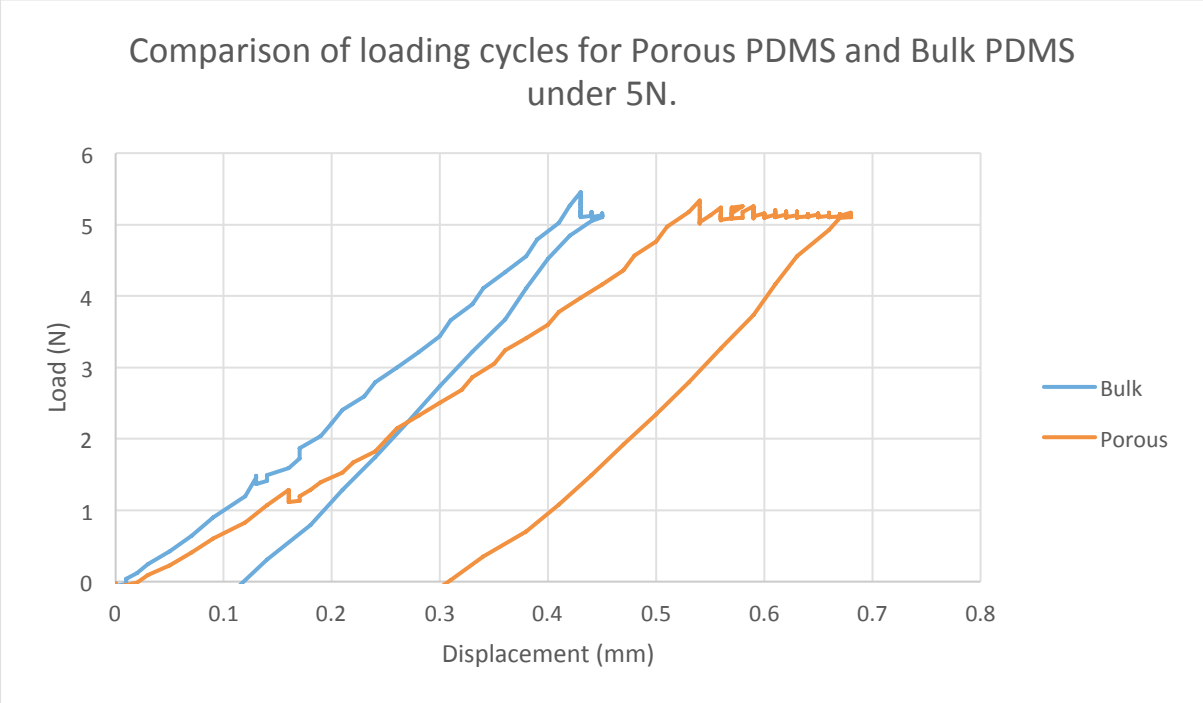

As seen in Figure 19 at around 0.55 mm when the test load of 5N is achieved the displacement continues to increase to maintain the load in contrast to the bulk sample where it is seen to be constant. This is confirmation that the sample has a good porosity and the lubricant is supporting the load within the pores, although as the lubricant is not pressurised to stay within the pores it is being displaced and the sample continues to be deformed.

The following results figures 20 through 32 show the displacement against time graphs for the various configurations tested. These results show more clearly how the displacement of the indenter had to be modified to keep a constant load over the time of the experiment. These results are especially useful for categorising the porous samples and seeing how they deform over time. The results also show the difference in the lubricants and how they affect the characteristic properties of each sample.

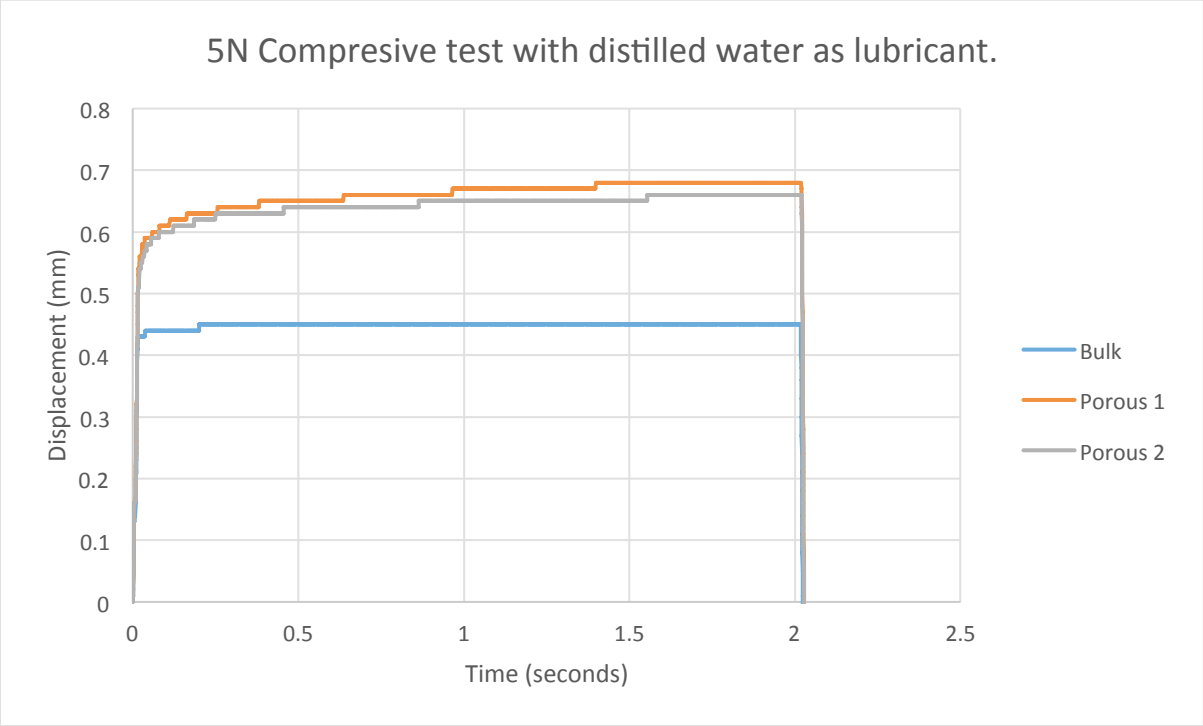

Figure 20. Comparison of porous and bulk samples with water as lubricant under compression of 5N.

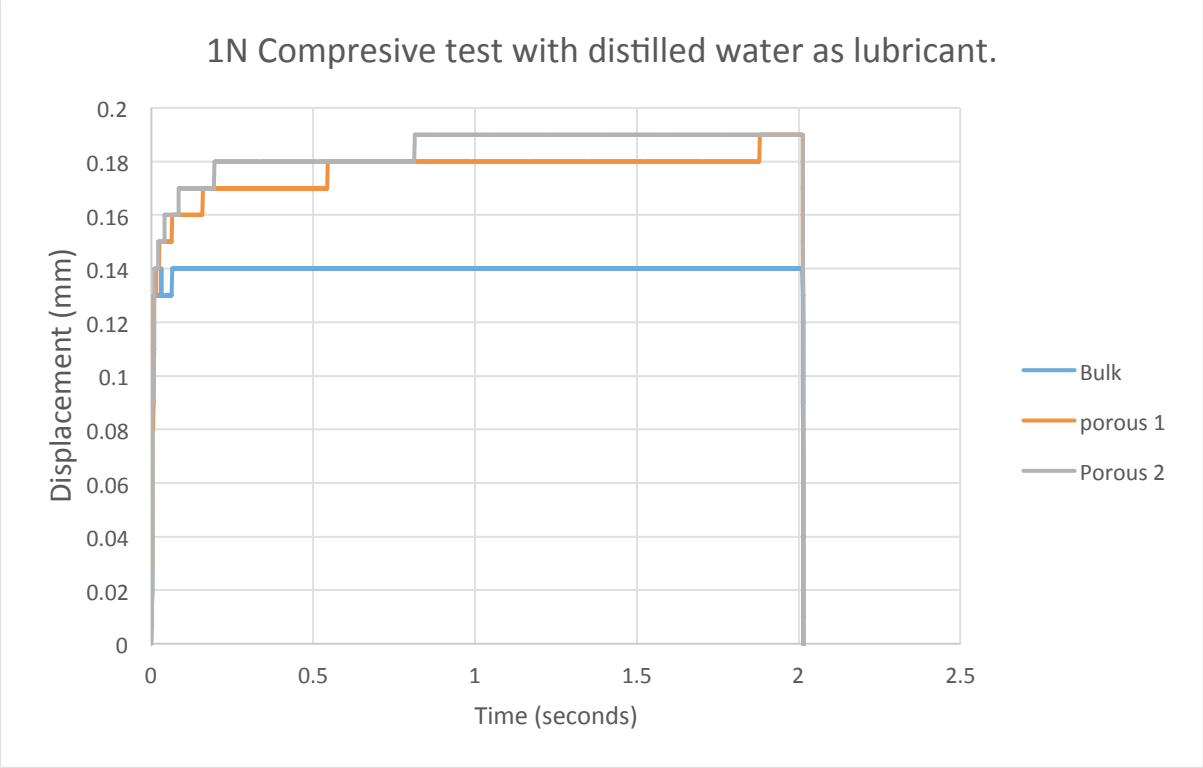

Figure 21. Comparison of porous and bulk samples with water as lubricant under compression of 1N.

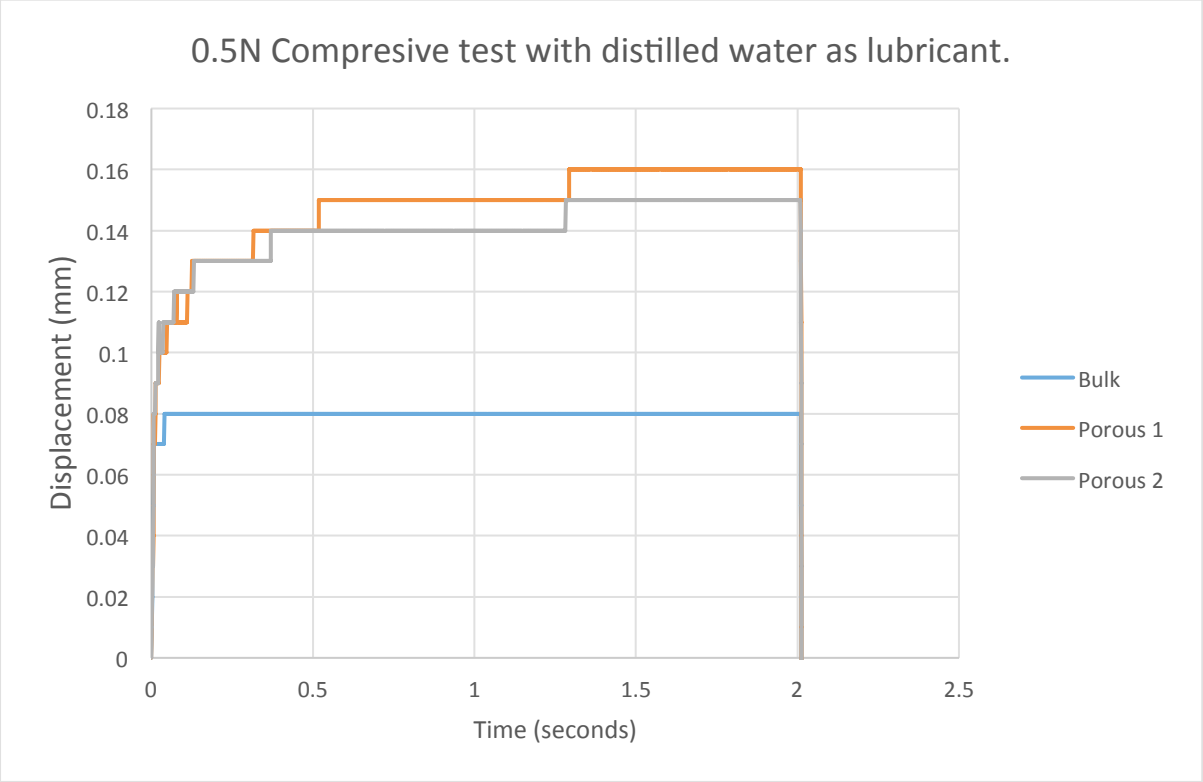

Figure 22. Comparison of porous and bulk samples with water as lubricant under compression of 0.5N.

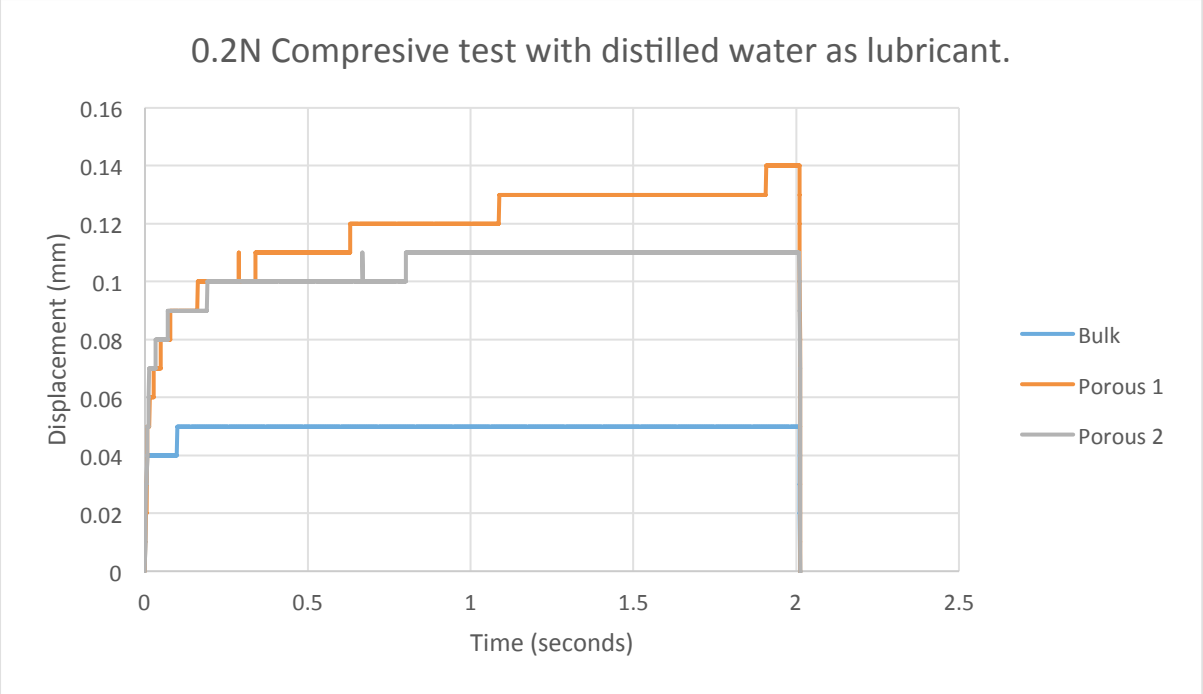

Figure 23. Comparison of porous and bulk samples with water as lubricant under compression of 0.1N.

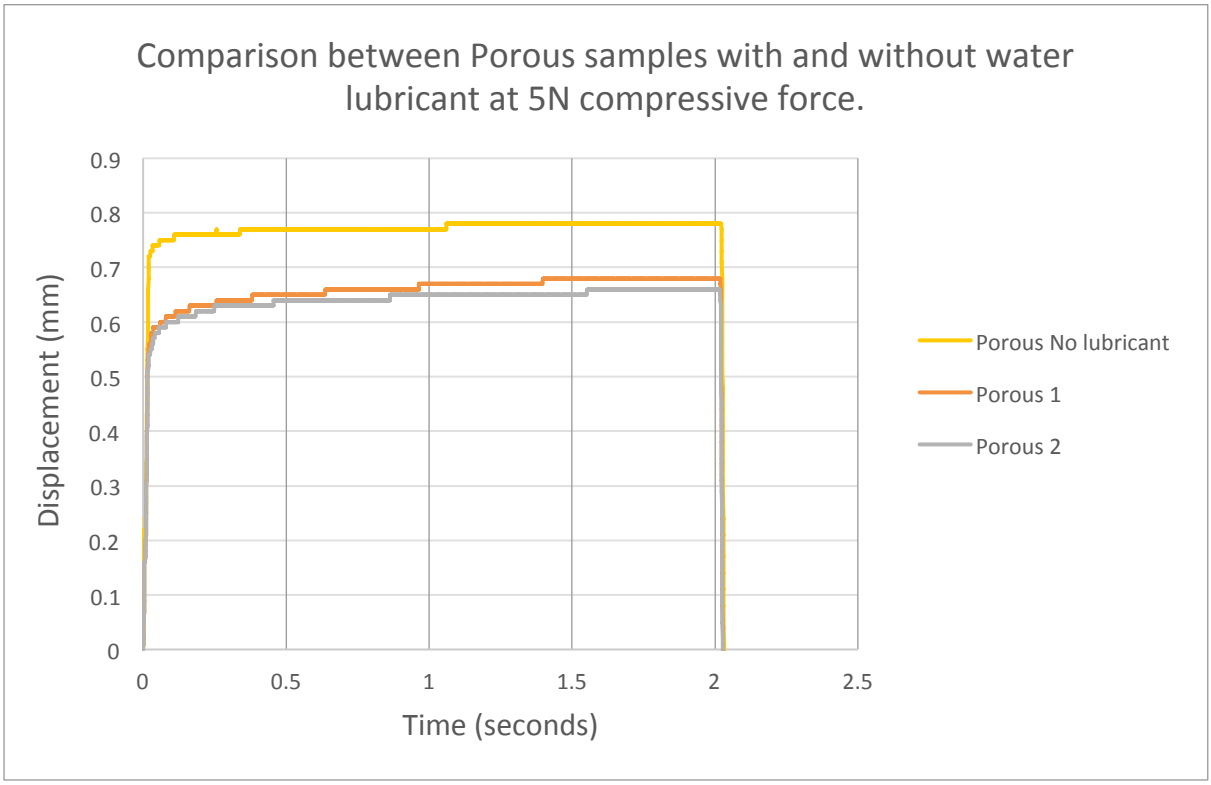

Figure 24. Comparison of porous samples with water as lubricant and without lubricant under compression of 5N.

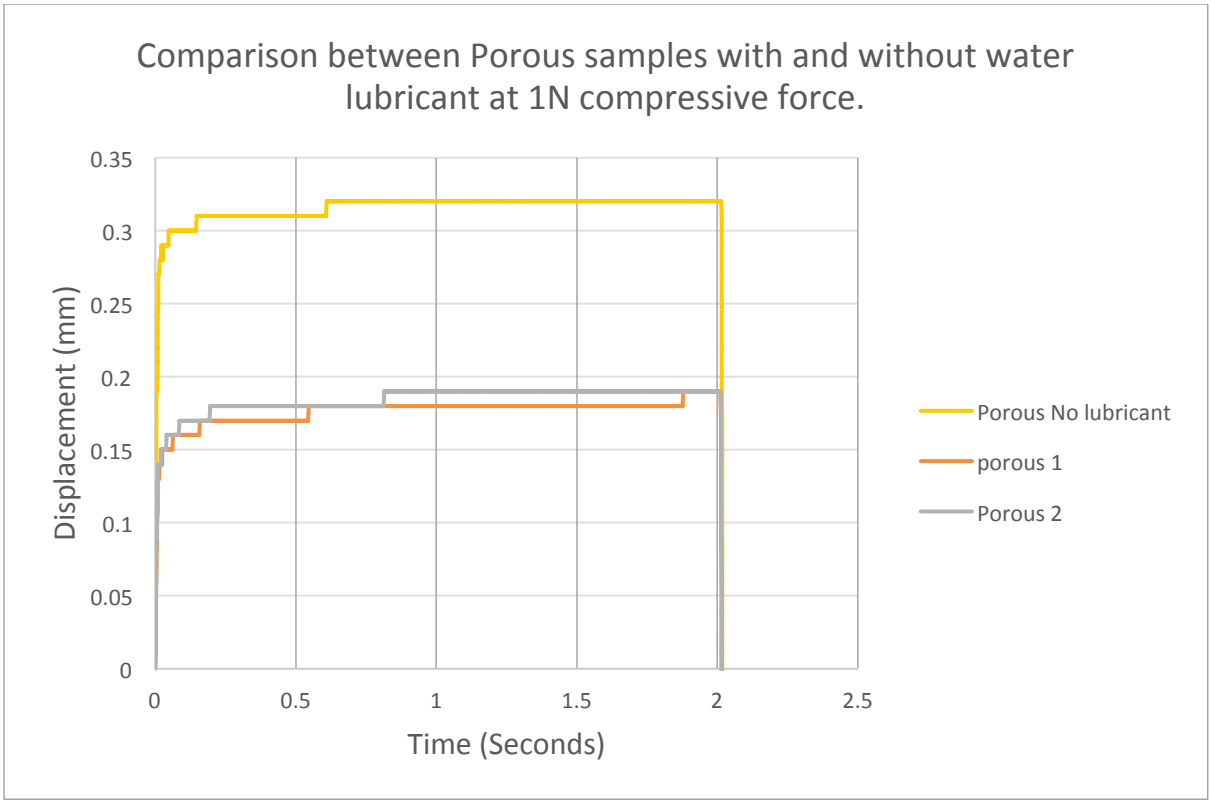

Figure 25. Comparison of porous samples with water as lubricant and without lubricant under compression of 1N.

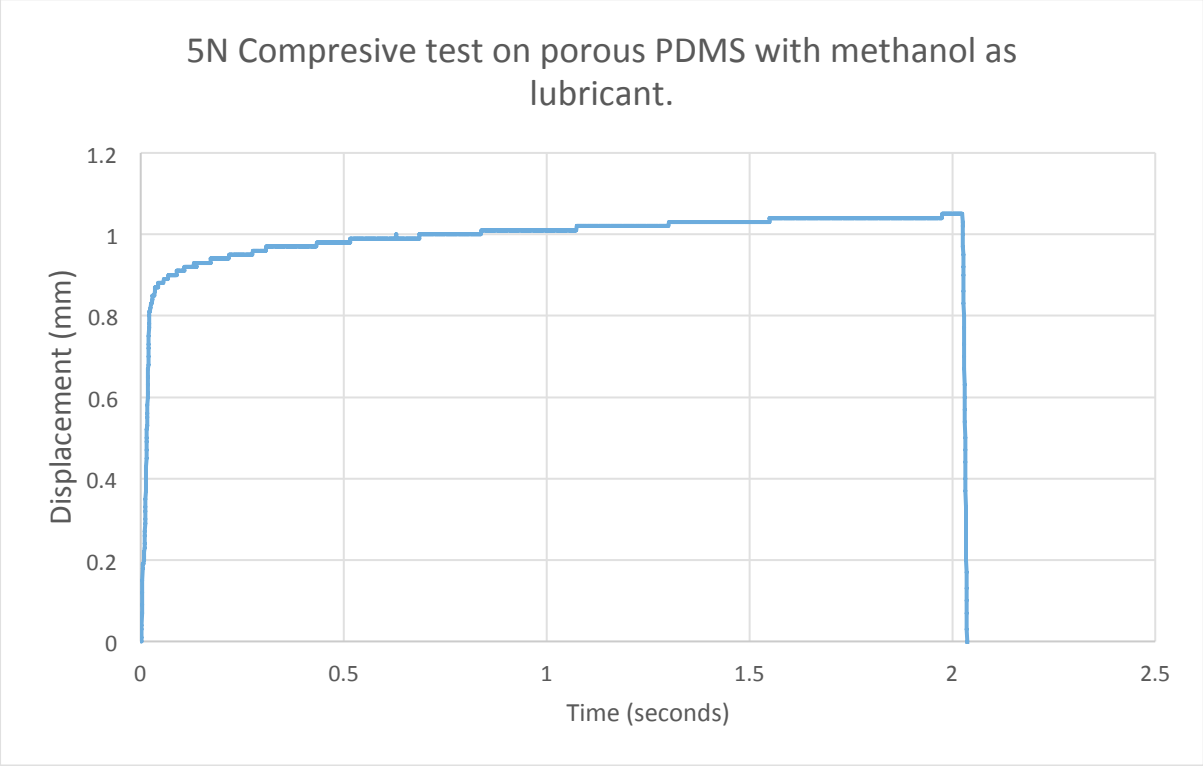

Figure 26. *Compression test of Porous PDMS with methanol as lubricant at a force of 5N.*

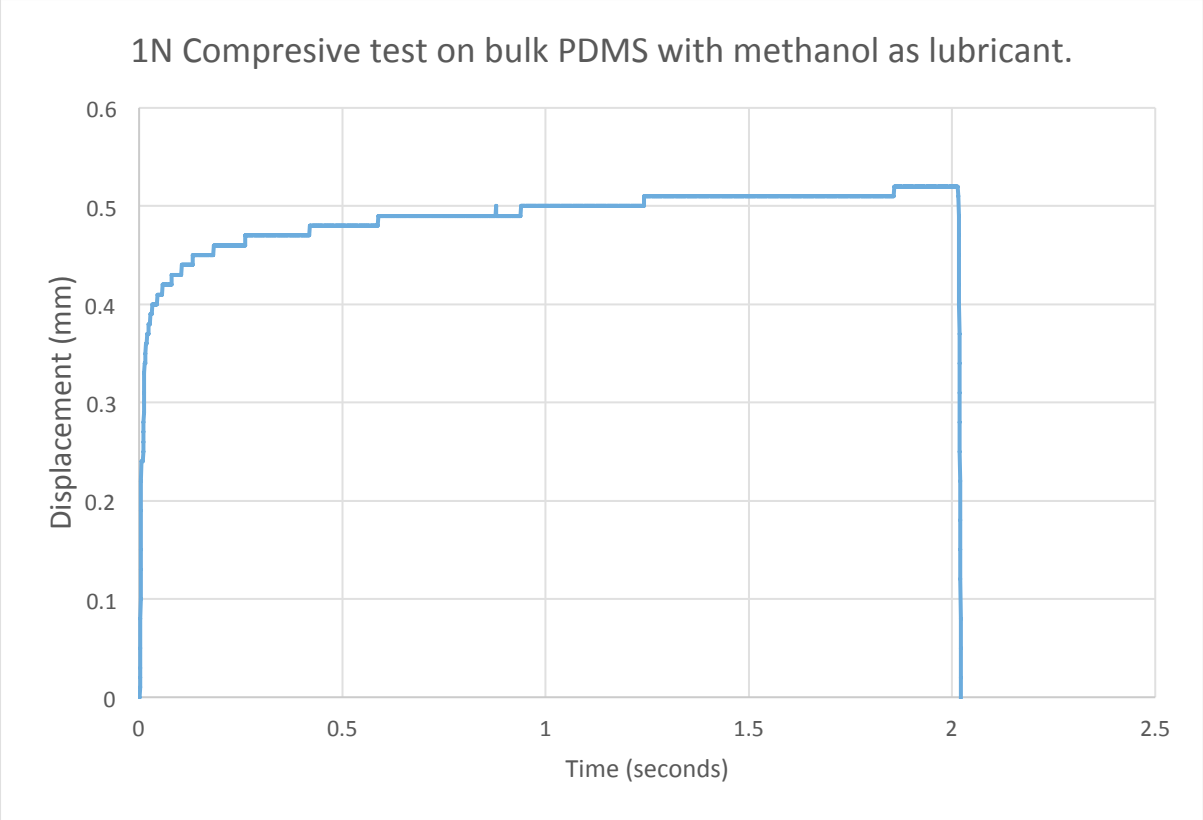

Figure 27. Compression test of Porous PDMS with methanol as lubricant at a force of 1N.

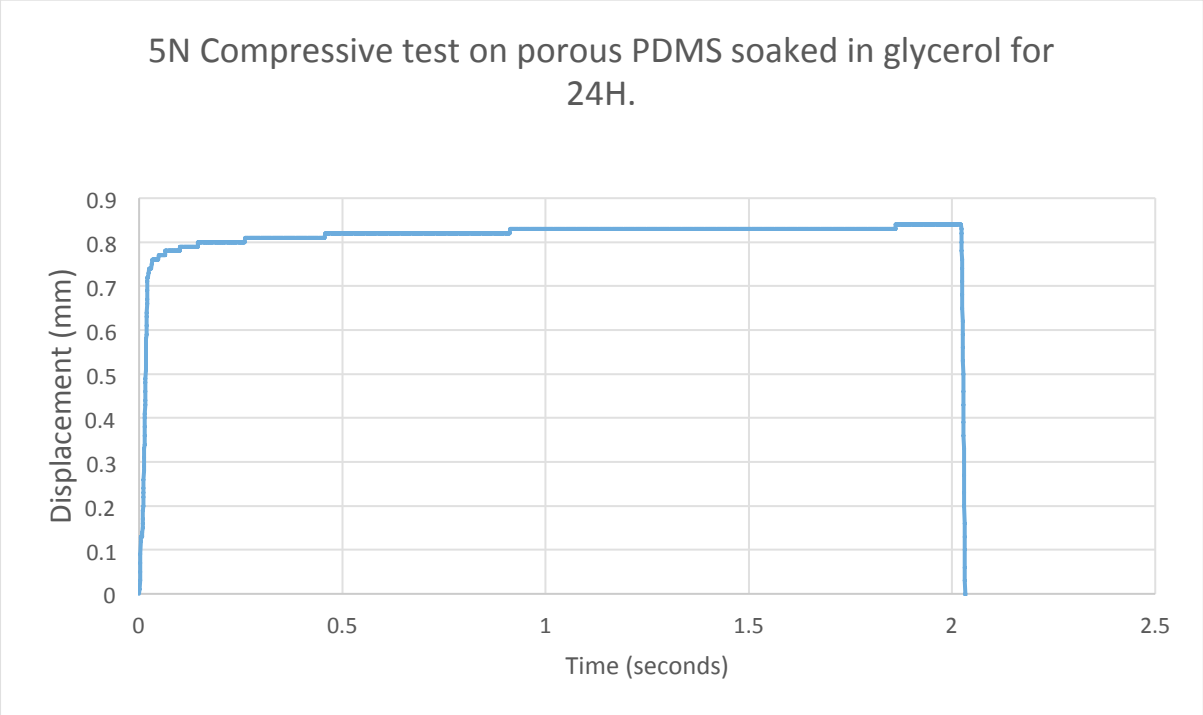

Figure 28. ***Compression test of Porous PDMS soaked in glycerol for 24h with glycerol as lubricant at a force of 5N.***

Figure 11:

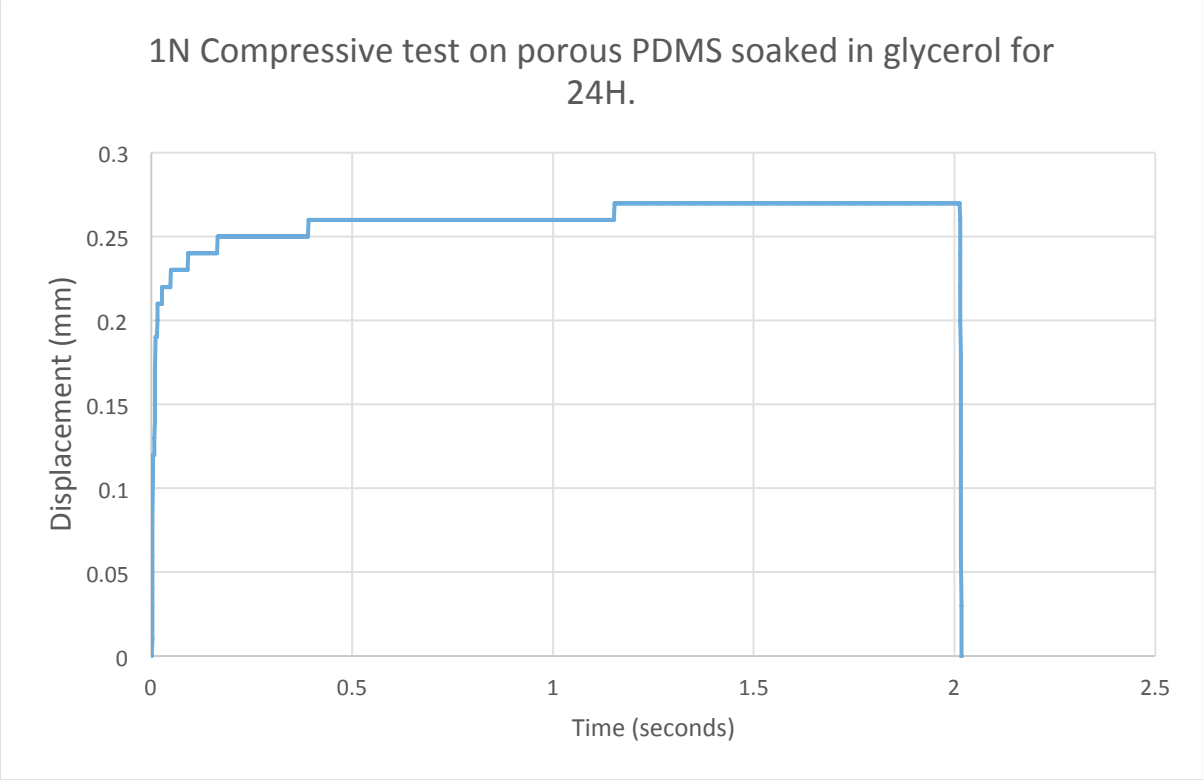

Figure 29. Compression test of Porous PDMS soaked in glycerol for 24h with glycerol as lubricant at a force of 1N.

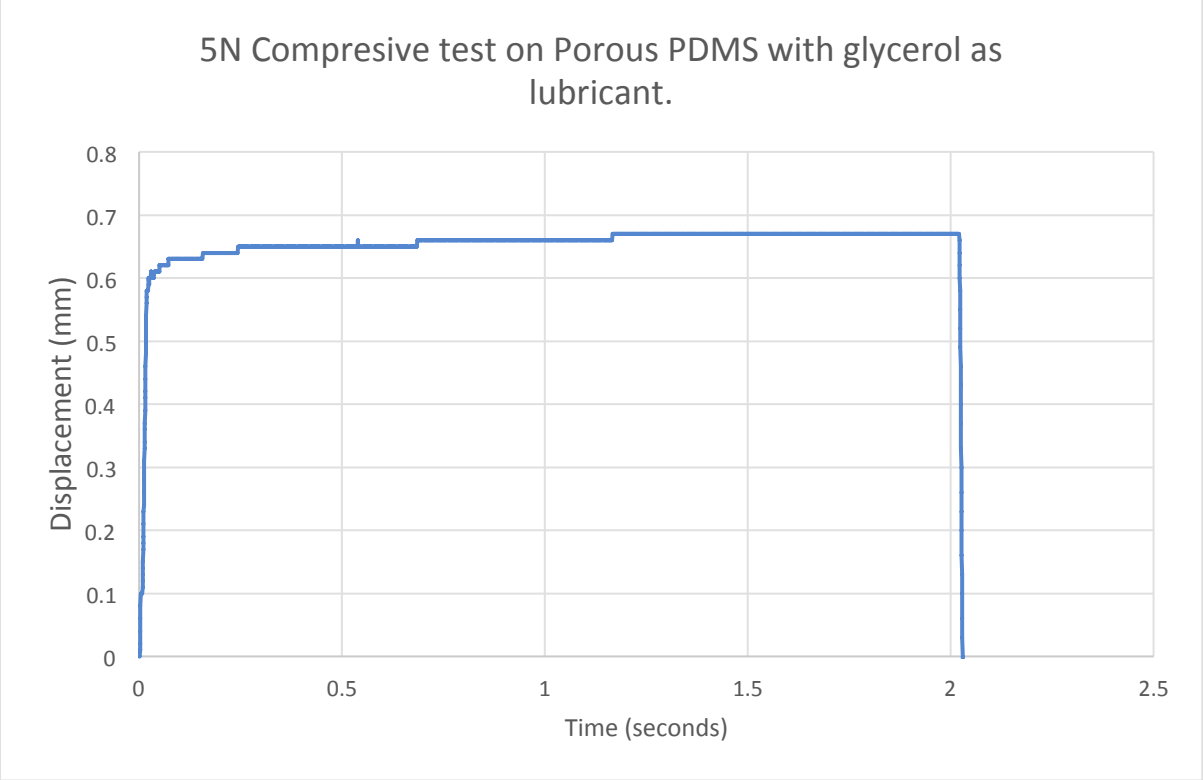

Figure 30. Compression test of Porous PDMS with glycerol as lubricant at a force of 5N.

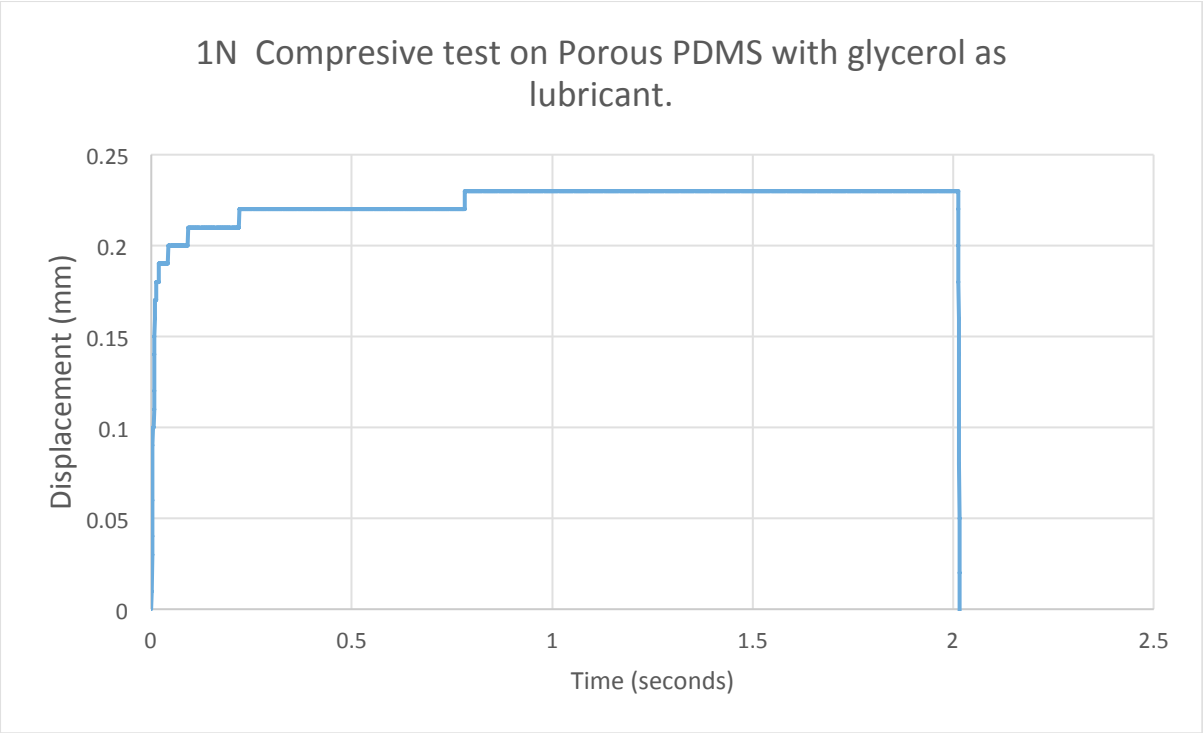

Figure 31. Compression test of Porous PDMS with glycerol as lubricant at a force of 1N.

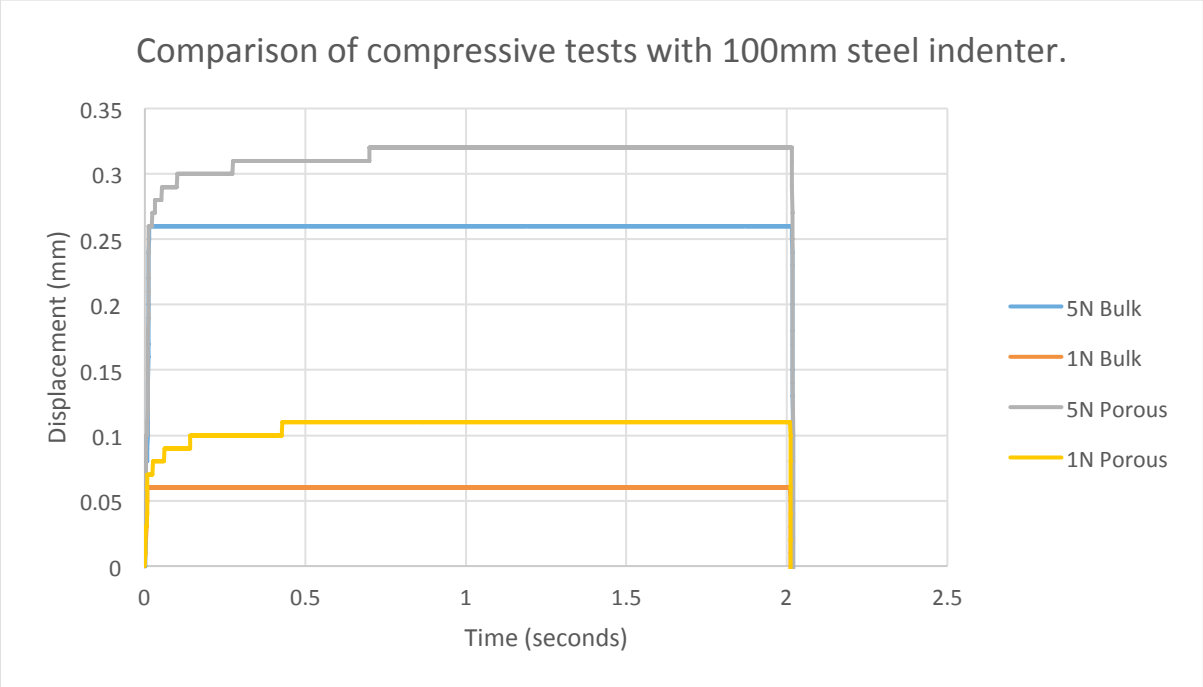

Figure 32. Comparison of porous and bulk PDMS at 1N and 5N with steel indenter (diameter 100mm)

Discussion

Initially looking at Figure 20 and Figure 21 it is seen that the higher load of 5n displaces the samples more than the 1N load, as expected. The bulk samples on both figures react in the way established above when looking at the loading cycles; reaching a maximum displacement before staying constant until unload. However, when looking at the porous samples the 5N force reaches an almost constant value much faster than the 1N test. The 5N test levels out at around 0.5 seconds whereas the 1N test levels off at around 1 second. Further to this as the load is reduced more to 0.5N and 0.2N in figures 5 and 6 respectively the levelling off stage occurs much later in the cycle. For the 0.5N test this occurs at 1.5 seconds and the 0.2N test at approximately 2 seconds. These results indicate that the porous samples are more effective at supporting the load through the lubricant trapped within the pores at lower loads compared to high loads. This is logical as at higher loads the pores are compressed more and therefore the lubricant is expelled from the pores before being able to support the load.

Figure 24 and Figure 25 show the comparison of the porous samples with water lubricant compared to porous samples with no lubricant. These results show how the porous samples deform significantly more when no lubricant is present. This shows further evidence that the lubricant plays a significant role in supporting the load. Agreeing with the previous results these figures also show that the porous samples are much more effective at the lower loads. The water-lubricated porous samples in figure 8 at the 0.2N load show half as much deformation as the non-lubricated samples at the same load.

Figure 26 and Figure 27 show the compressive test for porous PDMS samples but with methanol as the lubricant. Methanol is less dense than water with a density of 0.8g/cm$^{3(16)}$, compared to water with a density of 1g/cm^3 (17). The results are very similar to the water lubricated samples with a small increase in the total displacement. The 1N test does level off a little later than the water lubricated sample at the same load. The overall difference in displacement is highly likely to be due to difference in the samples during manufacture. The increase in time for the sample to level off could be due to the use of methanol opposed to water, PDMS is inherently hydrophobic and therefore the water lubricant is more likely to be expelled, whereas the methanol would have saturated the sample more easily and consequently could support more of the load throughout loading of the sample.

Figures 28, 29, 30 and 31 show the compressive tests for the porous samples with glycerol as the lubricant. Figures 28 and 29 have been soaked in glycerol for 24h before testing to saturate the samples pores. Glycerol is the densest lubricant tested with a density of 1.3g/cm$^{3(18)}$. The glycerol

results that have been soaked for 24h, don't show considerable change from the other glycerol samples, this indicates that the prolonged exposure to the glycerol does not increase saturation of the pores.

Looking at all the results the effectiveness of the lubricant seems to depend on how hydrophilic or hydrophobic it is, further work would be needed to identify the most appropriate lubricant for the PDMS samples. Another approach would be to make the samples from a different elastomer, or treat the surface to try and produce hydrophilic conditions.

Figure 15 shows the results for the porous and bulk samples with a water lubricant but with a different indentation tip. A steel indentation tip of 100mm diameter was used to create a flatter contact. Thus, the displacements are much lower as would be expected with a smaller average contact pressure. The characteristics of the porous samples compared to the bulk samples are the same as when testing with the smaller silicon nitride indenter tip.

4 Experimental

4.1 Sample Preparation

Fabricate, optimise and characterise a polydimethylsiloxane (PDMS) interconnected porous elastomer by using a microsphere templating method. Two methods to produce the microsphere templates were investigated and the optimal method chosen for further testing.

4.1.1 Heat Sintering (HS) method

Polymethyl methacrylate (PMMA) beads are added to a cylindrical aluminium well (internal diameter 25mm), with a glass bottom surface. The beads are packed by lightly tapping the well. The wells are put into an oven and the beads are sintered for 22 hours at 150°C.

4.1.2 Chemical sintering (CS) method

PMMA beads are suspended in a sintering solution of 1% acetone in 70% ethanol. The solution is then added to an aluminium well and incubated for 1-2 hours at 37°C to dry.

4.1.3 Addition of PDMS elastomer to porous PMMA templates

Once the microsphere templates had been created by sintering the PMMA beads the elastomer was added to the sample. PDMS polymer (Sylgard® 184 silicone elastomer, two part kit) was used as the elastomer. The PDMS polymer was prepared in a 10:1 ratio (10g of Base and 1g of curing agent) and vacuumed for 1 hour to remove the air bubbles. The elastomer samples were then added to the wells of the sintered PMMA beads and vacuumed for a further 30 minutes to remove any further air bubbles that may have formed, before curing in an oven at 55°C for 2 hours. This process was carried out for both the heat sintered and chemically sintered PMMA beads.

It has been considered that the samples may need to be centrifuged to ensure uniform penetration of PDMS within the microsphere template before curing. Centrifuging would occur at 500g for 5 mins at 4°C. However unless surface analysis of the samples show that this is required this step will be omitted, to expedite the preparation process.

4.1.4 Dissolving out the PMMA beads

Once the elastomer had cured the PMMA beads were removed by dissolving them out of the sample, so that only the porous structure of the elastomer would remain.

Samples were initially dissolved in acetone, and left at room temperature for 48 hours. On analysis of the samples using the optical microscope, a porous structure was not present therefore suggesting that the beads had not dissolved.

The samples were also dissolved in dichloromethane (DCM) and dimethylformamide (DMF) for 48 hours. DMF was the most promising and all the PMMA beads were dissolved out of the PDMS elastomer to create a porous structure.

Once the porous network had been established, the samples were placed in an aqueous lubricant – water and glycerol – and indentation and friction tests were completed.

4.2 Tribological Testing

Initial tribological tests were conducted using a bespoke low load tribometer using a spherical silicon nitride tip of diameter 1.25cm, with loads ranging from 1-10N. This tribometer utilized a SMAC Linear Slide Actuator, model LAL95-015-85F, controlled by LCC Control Center software with data recorded on LabView. Tests were conducted with a load of 3.2N and a sliding speed of 4.4cm/s.

Subsequent tests were then carried out with an Anton Paar NTR^3 table top nano-tribometer using a spherical ruby tip of diameter 2mm controlled by proprietary Anton Paar software, with data collected by the same software. The cantilever used was high resolution, with standard range of frictional coefficients. Tests were conducted with various loads and sliding speeds.

Due to the hydrophobic nature of PDMS, plasma treatment was used as a technique to hydrophilize the PDMS surface and encourage significant penetration of water into the micropores. The samples were placed in a Gala Instument Plasma Prep2 for 2 minutes. Glycerol (VWR Chemicals) was also used as a lubricant as it is compatible with PDMS and also has a higher viscosity.

4.3 Indentation testing

Initial material characteristic tests were carried out using a Mecmesin indenter with a hemispherical silicon nitride tip (diameter 12.5mm). The samples were tested at loads ranging from 0.2N – 5N. This system utilised a bespoke programme written on LabVIEW to conduct each test in a controlled and repeatable manner. The samples were tested in a range of lubricant mediums including water, methanol and glycerol. Some of the samples were left for extended times to soak in different lubricant mediums before being tested to increase the saturation of the porous samples.

The samples were placed and secured in glass petri dishes, the liquid medium was then added to cover each of the samples. Then indentation programme started with the indenter prepositioned within the test medium. The programme then applied a 0.1N pre-load to each sample before increasing the load to a specified force. The programme maintained this force for 2 minutes as the sample deformation was recorded via displacement of the indenter. The displacement was zeroed after the pre-load was applied to produce a datum point to allow the results of each test to be compared directly to one another.

Subsequent tests were conducted with a flatter hemispherical indenter tip made from steel (100mm curvature radius). These tests were carried out at loads of 1N and 5N. The tests were conducted on the same indenter as before with the only change being the size and material of the indenter tip.

5 Conclusions and Further Work

Conclusions

Overall, the formation of porous polymeric materials using PMMA beads and PDMS elastomer is promising. The method described above created a porous PDMS elastomer network, which can then be tested under load with a suitable aqueous lubricant. The method for producing the porous elastomers can be improved in order to create uniform pores. The PMMA beads could be sieved prior to heat sintering, so that the pore sizes are consistent throughout the sample and work could be done to potentially find an alternative elastomer.

With either glycerol or water used as the lubricant the porous samples had higher frictional coefficients than the bulk samples. This is likely due to the increased surface roughness and higher conformity of the contact for the porous samples.

Using glycerol decreased the frictional coefficient for the porous samples compared to water. This is due to the high porosity of the porous samples. As shown in the poroelastic theory reducing porosity or increasing the fluid viscosity increases the load capacity. Therefore the higher viscosity of the glycerol increases the load capacity of the porous samples compared to water, and thus reduces friction as the fluid phase supports more of the load. In order to reduce the friction of the porous samples below that of the bulk samples the porosity of the samples would need to be decreased, or alternatively a more viscous lubricant should be used.

Further Work

Although a heat sintering method with PMMA beads, followed by the addition of an elastomer is shown to be a suitable method of manufacturing a porous elastic structure, an alternative method that could be used is a 3D printing technique. A porous structure at this length scale using additive manufacture is however complex and requires further investigation into its viability.

To create a uniform porous elastomer, PMMA beads will first have to be sieved prior to heat sintering. Two sieves can be used to separate beads of a certain size, producing a more uniform template and thus a more uniform porous elastic structure.

References

1. Nebraska, U.o. *How Materials Carry Load.* [Online]. 2000. [Accessed 1st February 2017]. Available from: http://emweb.unl.edu/NEGAHBAN/Em325/01-How-Materials-carry-load/How%20Materials%20Carry%20Load.htm
2. Hu, R., Hewson, R., Morina, A. and Liu, Z. Influence of material properties and operating conditions on the predicted performance of poroelastic faced bearings. *Proceedings of the Institution of Mechanical Engineers, Part J: Journal of Engineering Tribology.* 2013, **228**(2), pp.131-139.
3. Haque, M.A., Kurokawa, T. and Gong, J.P. Super tough double network hydrogels and their application as biomaterials. *Polymer.* 2012, **53**(9), pp.1805-1822.
4. Nigam, K.M., Manohar, K. and Jaggi, S. Micropolar fluid film lubrication between two parallel plates with reference to human joints. *International Journal of Mechanical Sciences.* 1982, **24**(11), pp.661-671.
5. Bujurke, N.M., Kudenatti, R.B. and Awati, V.B. Effect of surface roughness on squeeze film poroelastic bearings with special reference to synovial joints. *Math Biosci.* 2007, **209**(1), pp.76-89.
6. Khosla, T., Cremaldi, J., Erickson, J.S. and Pesika, N.S. Load-Induced Hydrodynamic Lubrication of Porous Films. *ACS Appl Mater Interfaces.* 2015, **7**(32), pp.17587-17591.
7. Detournay, E. and Cheng, A.H.D. *Fundamentals of poroelasticity.* Pergamon, 1993.
8. Bujurke, N.M. and Kudenatti, R.B. An analysis of rough poroelastic bearings with reference to lubrication mechanism of synovial joints. *Applied Mathematics and Computation.* 2006, **178**(2), pp.309-320.
9. Naduvinamani, N.B. and Katti, S.G. Micropolar Fluid Poro-Elastic Squeeze Film Lubrication between a Cylinder and a Rough Flat Plate ^|^mdash; A Special Reference to Synovial Joint Lubrication. *Tribology Online.* 2014, **9**(1), pp.21-30.
10. Rohman, G., Lauprêtre, F., Boileau, S., Guérin, P. and Grande, D. Poly(d,l-lactide)/poly(methyl methacrylate) interpenetrating polymer networks: Synthesis, characterization, and use as precursors to porous polymeric materials. *Polymer.* 2007, **48**(24), pp.7017-7028.
11. Hong, Y., Zhou, J.G. and Yao, D. Fabrication of Interconnected Porous Elastomers by a Microsphere-Templating Process. *Advances in Polymer Technology.* 2013, **32**(1), pp.n/a-n/a.
12. Cam, C. and Segura, T. Chemical sintering generates uniform porous hyaluronic acid hydrogels. *Acta Biomater.* 2014, **10**(1), pp.205-213.
13. Tan, S.H., Nguyen, N.T., Chua, Y.C. and Kang, T.G. Oxygen plasma treatment for reducing hydrophobicity of a sealed polydimethylsiloxane microchannel. *Biomicrofluidics.* 2010, **4**(3), p.32204.
14. He, B., Chen, W. and Wang, Q.J. Friction and Wettability of a Micro-Textured Elastomer: Poly(Dimethylsiloxane) (PDMS). 2006, pp.1053-1062.
15. T Khosla, J.C., J.S Erickson and N.S Pesika. Hydrodynamic Lubrication of Porous Films. Applied materials and Interfaces. (pp.17586-17591).
16. *Methanol.* 2015. Available from: http://www.chemspider.com/Chemical-Structure.864.html
17. *H20.* 2015. Available from: http://www.chemspider.com/Chemical-Structure.937.html
18. *Glycerol.* 2015. Available from: http://www.chemspider.com/Chemical-Structure.733.html